SIGNAL PROCESSING WITHIN AND BETWEEN BACTERIAL CHEMORECEPTORS

A Dissertation

by

RUNZHI LAI

Submitted to the Office of Graduate Studies of
Texas A&M University
in partial fulfillment of the requirements for the degree of

DOCTOR OF PHILOSOPHY

May 2007

Major Subject: Microbiology

SIGNAL PROCESSING WITHIN AND BETWEEN BACTERIAL CHEMORECEPTORS

A Dissertation

by

RUNZHI LAI

Submitted to the Office of Graduate Studies of
Texas A&M University
in partial fulfillment of the requirements for the degree of

DOCTOR OF PHILOSOPHY

Approved by:

Chair of Committee,	Michael D. Manson
Committee Members,	Michael J. Benedik
	Frank M. Raushel
	Jin Xiong
Head of Department,	Vincent M. Cassone

May 2007

Major Subject: Microbiology

ABSTRACT

Signal Processing within and between Bacterial Chemoreceptors. (May 2007)

Runzhi Lai,

B.S., Huazhong Agricultural University, P. R. China

Chair of Advisory Committee: Dr. Michael D. Manson

The key control step in *E. coli* chemotaxis is regulation of CheA kinase activity by a set of four transmembrane chemoreceptors. The receptor dimers can form trimeric complexes (trimers of dimers), and these trimers can be joined by a bridge thought to consist of a CheW monomer, a CheA dimer, and a second CheW monomer. It has been proposed that trimers of receptor dimers may be joined by CheW-CheA dimer-CheW links to form an extended hexagonal lattice that may be the structural basis of the chemoreceptor patches seen in *E. coli*. The receptor/CheA/CheW ternary complex is a membrane-spanning allosteric enzyme whose activity is regulated by protein interactions. The study presented in this dissertation investigated intermolecular and intramolecular interactions that affect the chemotactic signal processing. I have examined functional interactions between the serine receptor Tsr and the aspartate receptor Tar using a receptor coupled *in vitro* phosphorylation assay.

The results reveal the emergent properties of mixed receptor populations and emphasize their importance in the integrated signal processing that underlies bacterial chemotaxis. A mutational analysis of the extreme C-terminus (last fifty residues) of Tar is also presented. The results implicate the receptor C-terminus in maintenance of

baseline receptor activity and in attractant-induced transmembrane signaling. They also suggest how adaptive methylation might counteract the effects of attractant binding.

DEDICATION

This dissertation is dedicated to three people who shared with me the pain and the joy required to complete it. The first two persons are my parents, Guoding Lai and Jinglan Zhong, for their patience, financial aid, and inspiration during my enduring student career. The third is my wife, Qinglan Chen, who unconditionally supported me, who cared for my life without complaining, and who shared equally with me all the emotional and financial burdens. Without the support and understanding from them, I could never have finished this long journey.

ACKNOWLEDGEMENTS

I am grateful to my beloved mentor Dr. Michael Manson for his patient guidance and relentless mentoring. Throughout my doctoral work he encouraged me to develop independent and critical thinking. Without his mentoring, I could not be the person I am today. I will never forget his frequent quote, “The graveyards are full of indispensable men.” – by Charles de Gaulle.

I am also very grateful for having an exceptional doctoral committee and wish to thank Dr. Michael Benedik, Dr. James Hu, Dr. Frank Raushel, and Dr. Jin Xiong for their support and encouragement.

I also appreciate my “Mike Manson Friends” for their support, friendship, critics, and encouragement. I would especially thank Dr. Brian Cantwell and Dr. Roger Draheim, who shared many ideas, critiques, and joyful inter-experimental breaks with me. We together built an invincible 303 clan.

I would also like to thank Lily Bartoszek, who is the great woman behind my mentor, for her meticulous editing of my manuscripts and essays, and for her wonderful dinners.

TABLE OF CONTENTS

LIST OF FIGURES

FIGURE Page

LIST OF TABLES

CHAPTER I

INTRODUCTION

BACTERIAL CHEMOTAXIS

Escherichia coli is a Gram-negative bacterium, typically about 2 μm long and 0.8 μm wide. It is equipped with several bi-directional rotary motors that are embedded in the cell membrane and distributed randomly over the cell surface. The motor drives a long, helical, left-handed filament, and is powered by an electrochemical gradient of H^+ across the cytoplasmic membrane. The rotation of the flagella is the propelling force for the cells to swim in an aqueous environment. Counter-clockwise (CCW) rotation of the flagella causes the 4-7 filaments to form a left-hand helical bundle that propels the cell in a straight swim, termed a run (Figure 1.1) (*1*). The speed of the run can be up to 40 $\mu m \cdot s^{-1}$ *(2)*, which is 20 body lengths per second. Clockwise (CW) rotation of the flagella disrupts the bundle. As a result, the cell randomly reorients in an event termed a tumble. The next run will thus be in a new direction.

Flagellar motility gives *E. coli* advantages in competing for limited nutrients or avoiding harmful chemicals. In an isotonic environment, cells make short runs (a few seconds) punctuated by brief tumbles (around 0.1 second), resulting a 3-dimensional random walk (Figure 1.1) *(3)*. This movement is an accelerated version of Brownian

---

This dissertation follows the style of *Biochemistry*.

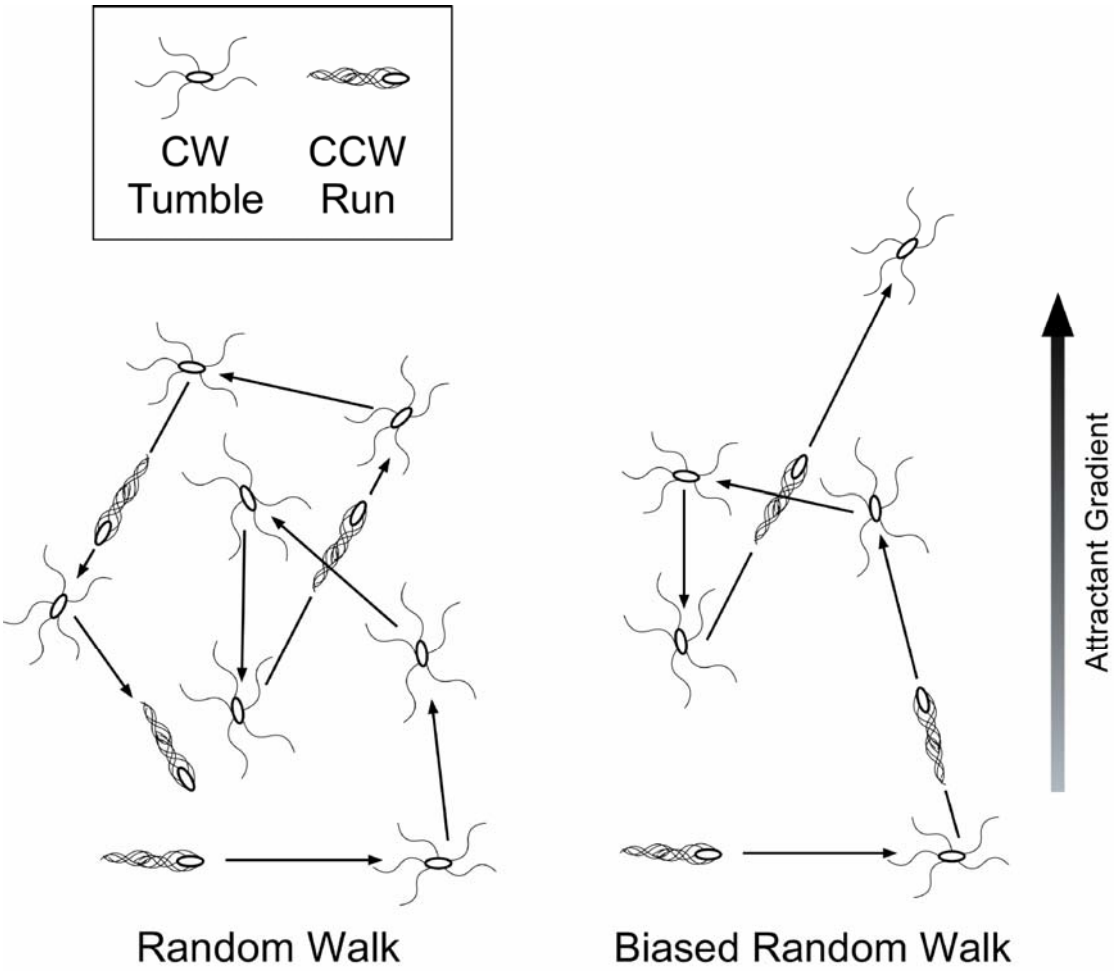

FIGURE 1.1 Behavior of an *E. coli* cell in an isotropic medium (left) and gradient of attractant (right). In either case, the cell swims in a straight line (runs), randomizes its direction by tumbling, runs again, tumbles, *etc*., yielding a three-dimensional random walk. The effect of an attractant gradient is to extend the mean duration of runs in an up-gradient direction; runs in the down-gradient direction are not appreciably shortened. The cell therefore exhibits a biased random walk and migrates in the up-gradient direction. The gradient is sensed by a temporal mechanism, in which the instantaneous concentration of attractant sensed by a cell is compared with the concentration sensed a few seconds previously.

motion. When the cell swims up an attractant gradient, it responds by decreasing the frequency of tumbling. The result is a prolonged run toward higher concentration of the attractant and migration up the gradient. In the presence of a repellent gradient, the frequency of tumbling is suppressed when the cell swims down the gradient. Because of tumbling, the migration speed is only a small fraction of the swimming speed, and the path of the cell describes a biased random walk (Figure 1.1). The paradigm of this run and tumble behavior can be applied to many other motile bacteria. The coupling of a sensory system to the cell motor enables the bacteria to move in gradients of light intensity (phototaxis), redox potential (aerotaxis), and temperature (thermotaxis), as well as in chemical gradient (chemotaxis) *(4-8)*.

Swimming is the one of the most characteristic behaviors of prokaryotic cells. It not only enables them to respond to the stimuli from the environment, it also distinguishes them as living entities. A molecule can diffuse across an *E. coli* cell in a few milliseconds, but the same molecule requires hundreds of seconds to move 1 mm. Thus, chemotactic movement enables cells to find new environments that are rich in nutrients or low in toxins faster than the chemicals can diffuse over long distances.

The molecular chemotactic machinery of *E. coli* has been investigated since the 1960s, in studies originally initiated by Julius Adler *(9-11)*. This system provides the best-known example of a cell-signaling network and sophisticated information processing. The understanding of bacterial chemotaxis has value beyond microbiology, playing a role in fields like ecology *(12)*, chemistry *(13)*, physics *(14)*, and even astronomy *(15)*.

THE CHEMOTACTIC SENSORY CIRCUIT

Chemicals in the environment are recognized in *E. coli* by one of a group of four closely related canonical Methyl-accepting Chemotaxis Proteins (MCPs) and a fifth MCP-like receptor. These receptors localize to the cytoplasmic membrane. Tar mediates attractant responses to L-aspartate and maltose, as does Tsr to L-serine. Trg senses ribose, glucose and galactose as attractants, Tap is responsible for chemotaxis toward di- and tripeptides, and Aer mediates aerotactic responses. The sugars and peptides are first recognized by periplasmic substrate-binding proteins, which interact with the periplasmic domain of the receptors only when the binding proteins are in their closed, ligand-bound form. Amino acids, in contrast, bind directly to the periplasmic domain of the homodimeric receptors at the subunit interface. Input signals perturb the sensory domain and cause conformational movements and signal transduction on a millisecond time-scale *(16)*.

Tar and Tsr are present in about 10-fold and 20-fold more copies per cell, respectively than Trg or Tap *(17, 18)*. Tar and Tsr are therefore referred to as high-abundance receptors, whereas Trg and Tap are called low-abundance receptors. The CheW coupling factor and the CheA histidine-protein kinase (HPK) interact with the membrane-distal tip of the cytoplasmic domain of receptors. The receptors stimulate the HPK activity of CheA 50 and 100 fold for Tar and Tsr, respectively. CheA uses ATP to phosphorylate itself on a histidinyl residue that is highly conserved in all HPKs. This phosphoryl group is then transferred to an aspartyl residue on the CheY protein, which is also highly conserved in the response regulators that are substrates for phosphotransfer

from HPKs. Spontaneous loss of the phosphoryl moiety of phospho-CheY is greatly accelerated by the CheZ phosphatase (Figure 1.2). Changes in the signals from the chemoreceptors shift the rate of CheY phosphorylation on a time-scale of tenths of a second *(16)*.

Phospho-CheY is the molecule that communicates between the receptors and the flagellar motor. The current model suggests that the larger the number of the 34 FliM proteins present in the switch complex of the motor that are occupied by phospho-CheY, the greater the probability that the motor will rotate CW *(19-22)*. The correlation between motor rotational bias and the cytoplasmic concentration of phospho-CheY describes a steep sigmoid curve *(22)*. The concentration range of phospho-CheY that enables the switch of CW/CCW rotation of the motor is ~2μM (2μM to 4μM), with the highest frequency of switching occurring at 3μM. This sensitive input-output relationship enables the signal to be amplified in the output. In an unstimulated cell, the competing activities of phosphotransfer from CheA and dephosphorylation by CheZ maintain phospho-CheY at a level that allows the cells to spend most of their time in runs, punctuated every few seconds by tumbles *(16)*.

Attractant ligands inhibit the activity of CheA associated with the relevant receptor to a level below the baseline value for free CheA. This process is called sequestering *(23)*. The consequence of this inhibition is that CheA autophosphorylation decreases, thereby reducing phosphotransfer to CheY. Phospho-CheY levels in the cell fall, and the probability of CW rotation falls.

A cell senses a spatial gradient by a temporal mechanism (Figure 1.2). In essence,

FIGURE 1.2 Bacterial chemotaxis system. Chemoreceptors are homodimers that form a complex with histidine-kinase CheA through the coupling protein CheW. CheA autophosphorylation activity is stimulated in the complex, and the phosphoryl group is transferred to the CheY response regulator or the CheB methylesterase. Phospho-CheY binds to the FliM protein in the switch/motor complex and stimulates CW rotation. The methyltransferase CheR and the methylesterase phospho-CheB add and remove, respectively, methyl groups at specific glutamyl residues on in the receptors. Attractant binding to the receptor inhibits CheA activity, thereby decreasing the production of phospho-CheY and phospho-CheB. The autodephosphorylation of phospho-CheY is accelerated by the CheZ phosphatase. CheR continues to add methyl groups to the receptor, and the decrease in methylesterase activity accompanying the decrease in phospho-CheB results in increased methylation of the receptor. Since methylation enhances the CheA-stimulating activity of the receptor, this process compensates for the effect of attractant binding on CheA activity. A, B, R, W, Y, and Z represent CheA, CheB, CheR, CheW, CheY, and CheZ, respectively.

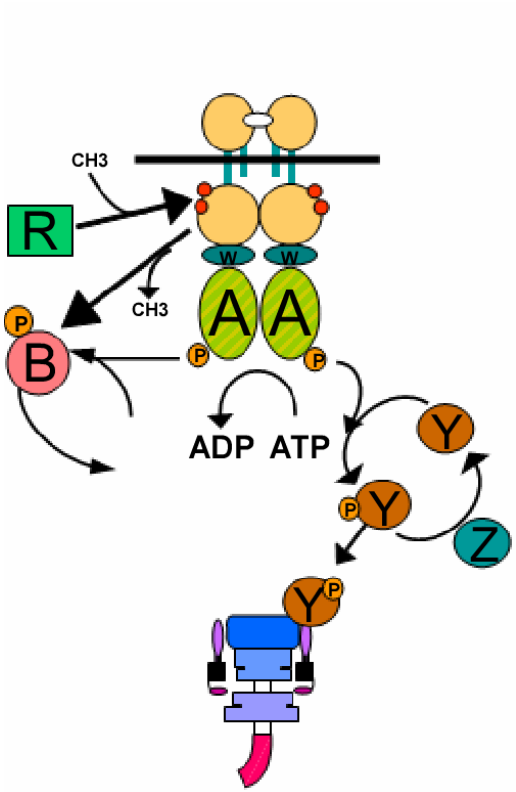

CW/CCW

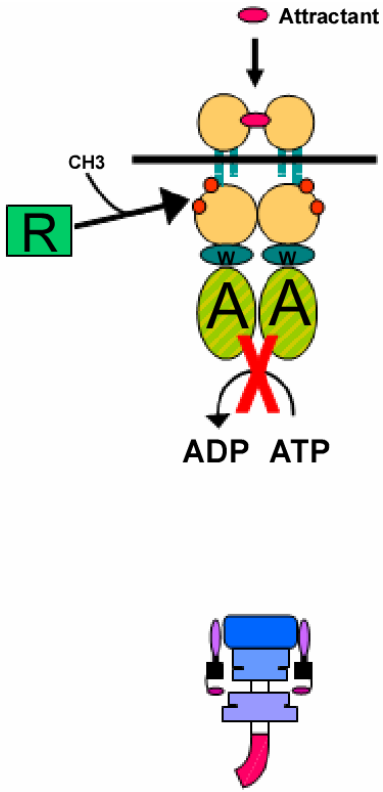

CCW

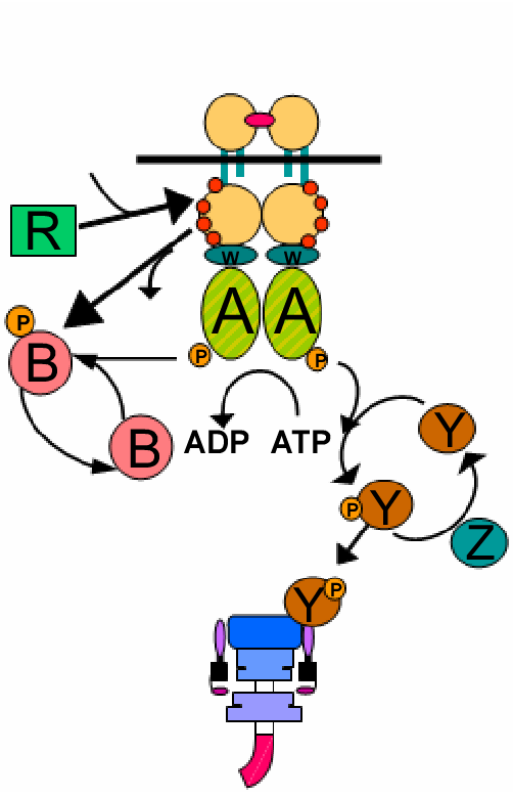

CW/CCW

it compares the instantaneous concentration, measured by the extent of receptor occupancy, against its "memory" of the concentration several seconds previously. This memory is made possible by adaptation through modulation of the methylation state of the receptors. Each receptor monomer contains from 4 to 6 glutamyl (E) residues that are substrates for methylation by the CheR methyltransferase, which uses S-adenosylmethionine as the methyl-group donor. Demethylation is carried out by the CheB methylesterase. CheB is active only when it is phosphorylated by CheA kinase. Methylated glutamyl residues (E^m) and glutaminyl residues (Q) have the same effect, which is to increase the CheA-stimulating activity of the receptor. Some of the methylation sites are originally translated as glutaminyl residues, which are subsequently deamidated by CheB. The four methylation sites of Tsr and Tar, for example, are synthesized in the QEQE configuration.

The methylation level of a ligand-bound receptor increases for two reasons. First, the drop in CheA activity leads to a decrease in the amount of phospho-CheB, which decays spontaneously with a half-life of seconds to lower the methylesterase activity relative to the methyltransferase activity. Second, the ligand-bound receptors become better substrates for methylation by CheR.

The effect of the increased methylation is to restore the original CheA-stimulating activity of the receptor, even when ligand remains bound, thereby bringing the levels of phospho-CheY and phospho-CheB back to pre-stimulus levels and restoring the normal ratio of running and tumbling. However, since the increase in methylation is slow (on the order of several seconds) relative to the inhibition of CheA and the drop in phospho-

CheY levels (less than 200 msec) *(24, 25)*, there is a brief time in which the cell will respond to increasing levels of attractant by suppressing tumbles. The differences in the time scales of CheA inhibition and adaptation serve as the "memory" mechanism for temporal sensing. Adaptation to small changes in attractant concentration can be achieved in 2 to 4 seconds *(26)*. In an artificial situation, large jump increases in attractant concentration can be imposed. Under these conditions, the smooth-swimming response to an attractant can last for many minutes until methylation catches up and the adapted cells start tumbling again.

The difference in adaptation times to large and small stimuli can be explained by methylation kinetics. Different methylation sites have different rates of methylation/demethylation by CheR/CheB. Small changes in ligand concentration can be balanced by small changes in methylation level. Furthermore, the higher the basal methylation level of a receptor, the slower its subsequent methylation. Therefore, adapation times correlate with the initial methylation levels of the receptors, which in turn reflect the signaling state of the receptors.

The consensus sequence of the methylation sites is Glu-Glu-X-X-Ala-Ser/Thr-X-Glu-Glu, in which the Glu residues that can be methylated are underlined. Because the methylation regions are in an extended coiled-coil helical bundle (Figure 1.3), which has a pitch of 3.5 residues per 360^{o} turn, this spacing of sites places them on the same helical face and makes them equally accessible to CheR and CheB.

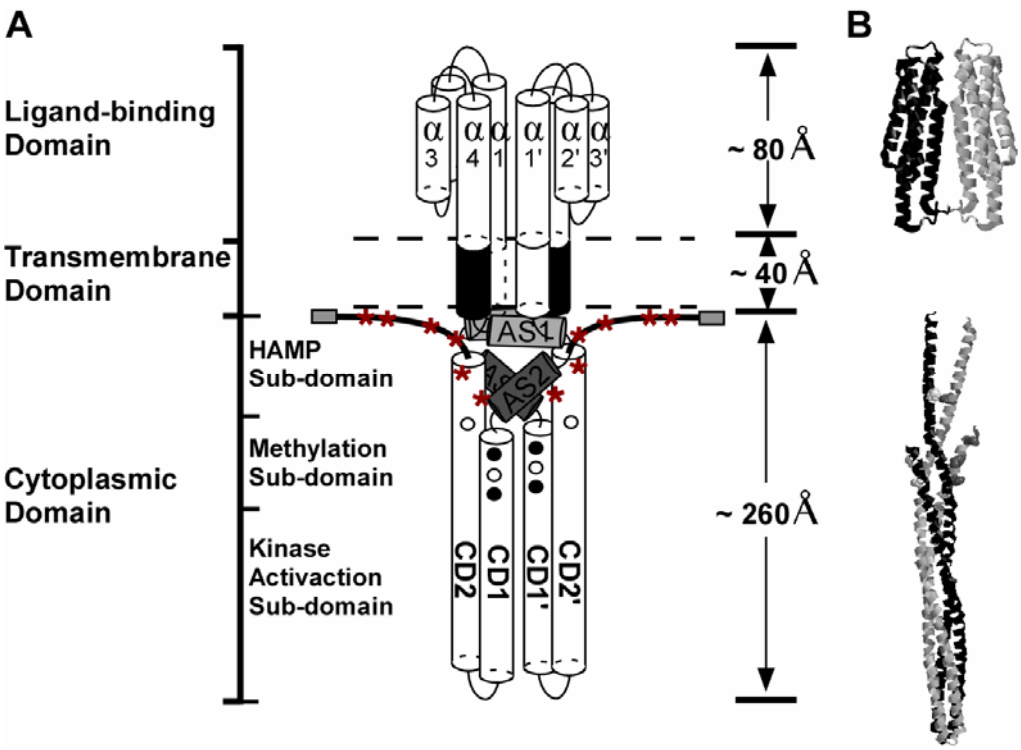

FIGURE 1.3 Model of an intact *E. coli* Tar chemoreceptor dimer. A, schematic diagram of the intact receptor dimer. The two dashed lines represent the membrane bilayer boundaries. Starting at the N-terminus, each monomer consists of transmembrane helix 1 (TM1, white); a periplasmic domain that is a four-helix bundle (α1 to α4); transmembrane helix 2 (TM2, black); a HAMP linker that consists of amphipathic helix 1 (AS1 light gray) and 2 (AS2, dark gray); a helical hairpin comprising the highly conserved adaptation and signaling region; and a disordered C-terminal tail (thick black line) with the NWETF CheR/B binding motif (gray box) at its end. The length of each domain is indicated at the right. B, ribbon diagram of the Tar periplasmic domain and the Tsr cytoplasmic hairpin. The dimensions are scaled to match those of the diagram model. One monomer is in black, the other in gray. Dark gray balls in the monomers mark methylation sites. The computer-modeled portions without crystallographic structures include TM1, TM2, HAMP, and residues 514 to 553.

REGULATION OF CHEMOTACTIC GENES EXPRESSION

There are ~60 genes that are involved in *E. coli* motility and chemotaxis, including genes for flagella, motility, and chemotactic sensing. These genes are clustered in three regions at 24, 42, and 43 min of the chromosome, respectively. Within each region, the genes are arranged in multiple operons. The Tar and Tap chemoreceptors are encoded in region II in an operon that also contains *cheRBYZ*. Trg and Tsr Chemoreceptors are products of single genes located at 31 and 99 min of the chromosome, respectively.

The expression of the chemotactic genes is regulated by a cascade control. The regulatory hierarchy responds to environmental stress and has three levels *(27, 28)*. Level 1 genes (*flhC* and *flhD*) are required for expression of level 2 genes and their expression is tightly regulated. The expression of FlhC and FlhD is under positive control of the cyclic AMP/CAP (catabolite activator protein) complex *(29)* and factors like temperature *(30)* and heat shock proteins *(31)*. It is also down-regulated by the level of OmpR, which is the response regulator of osmoregulation *(32)*. Besides regulating the expression of chemotactic level 2 genes, FlhDC also affects the cell growth and cell division *(33)*. Most level 2 genes encode flagellar components, basal body, and hook genes. Some of the level 2 genes are regulators for level 3 genes expression. One of them is a σ^{28} factor gene, *fliA*. It is required for the expression of level 3 genes. Another regulator gene is *flgM*, which encodes an anti-σ^{28} factor that inhibits the expression of level 3 genes. Upon completion of the flagellar hook-basal body complex, FlgM is transported out of the cell to initiate level 3 gene expression. The Che and MCP genes are in level 3 of the hierarchy.

STRUCTURE OF CHEMORECEPTORS

The four canonical MCPs (Tar, Tsr, Tap, and Trg) are stable homodimers in the presence or absence of ligand. Starting at the N-terminus, each receptor monomer consists of: transmembrane helix 1 (TM1); a periplasmic domain that is a four-helix bundle (α1 to α4); transmembrane helix 2 (TM2); a HAMP (histidine kinases, adenylyl cyclases, methyl binding proteins and phosphatases) linker that consists of amphipathic helices 1 (AS1) and 2 (AS2); a very long helical hairpin (CD1 and CD2) that comprises the highly conserved signaling region; and a disordered C-terminal tail with the NWETF CheR/B binding motif at its end (Figure 1.3). From the top of the periplasmic ligand-binding domain to the kinase interaction region is over 300 Å.

Crystal structures have been resolved separately for two cytoplasmic domains, HAMP and the long helical hairpin. The NMR structure study of a soluble archaeal HAMP domain of unknown function comprises a homodimeric, four-helix, parallel coiled-coil with knob-to-knob interhelical packing *(34)*. However, the structure was not determined in the presence of membrane or in the context of a full-length receptor. Thus, the structure possibly represents one signaling state that the HAMP domain can assume, a tight conformation with minimal-energy packing, without restraints imposed by other parts of the receptor.

An X-ray crystallographic study of the cytoplasmic domain of Tsr showed that it consists of a long coiled-coil with two antiparallel helices (CD1 and CD2) *(35)*. The cytoplasmic domains of a receptor dimer form a tight four-helical bundle. It has been proposed that the tight packing of the cytoplasmic domain corresponds to the “on” state

of the receptor, whereas the cytoplasmic domain is more dynamic in the "off" state.

A higher level structure was also revealed by the X-ray analysis of Tsr, and has been confirmed by genetic and cysteine-crosslinking studies *(36, 37)*. The receptor can form trimers of dimers (Figure 1.4), which probably are the basic units for receptor function. Through interaction at their highly conserved cytoplasmic tips, different chemoreceptor homodimers can form heterotrimers of dimers. Formation of heterotrimers of dimers formation was confirmed by analysis of compensating mutations affecting the tip of the Tar and Tsr cytoplasmic domains *(36, 38)*, and also by cysteine-crosslinking within trimers of dimers *(37, 39)*. This organization would bring different chemoreceptors into close physical contact.

As CD2 approaches the membrane, the peptide chain becomes an unstructured random coil starting at residue 514. At the C-terminal end of high-abundance MCPs there is a pentapeptide sequence (NWETF), which is missing in low-abundance MCPs. This pentapeptide serves as the binding site for CheR and CheB *(40-43)*. The unstructured carboxyl terminus (C-terminal tail) has been considered to be a flexible tether for the NWETF pentapeptide. However, the close proximity of the cell membrane and the HAMP domain to the C-terminus makes it tempting to speculate that the C-terminus may be involved in functional interactions during receptor signaling.

SIGNALING GAIN AND THE CHEMORECEPTOR LATTICE

The *E. coli* chemotactic system is a sensitive and robust model system for transmembrane signaling. It can detect and respond to a change in ligand concentration

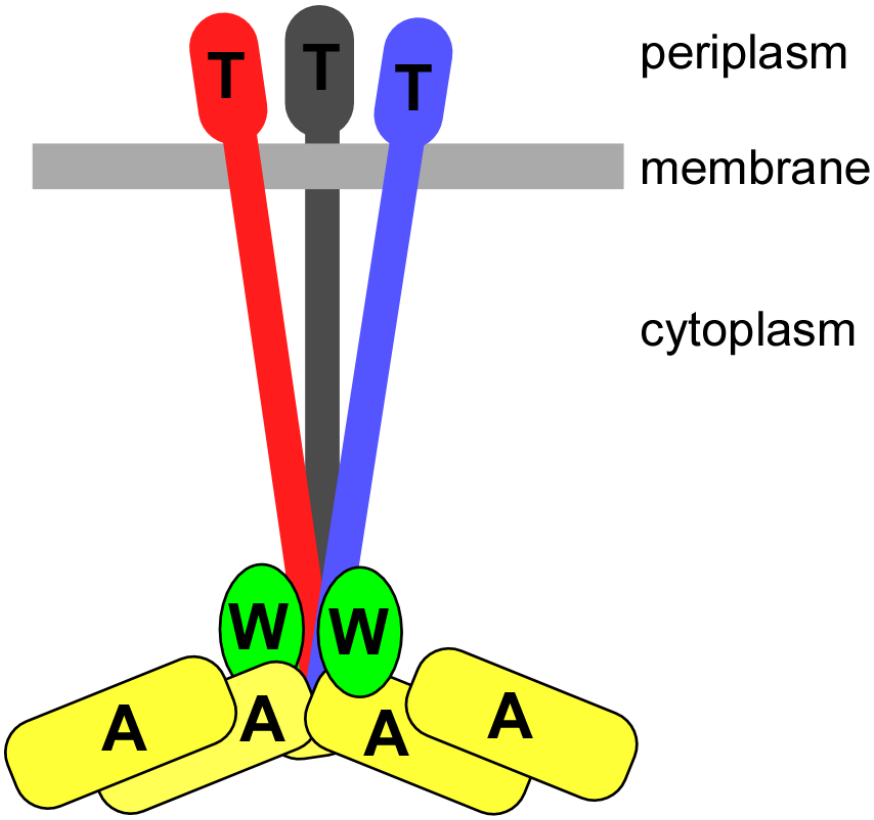

FIGURE 1.4 Schematic diagram of receptor trimer of dimers docked with CheA and CheW. Each receptor dimer (T) is shown in a different color. CheW (W) and CheA (A) are shown as green and yellow ovals, respectively. CheA is shown as a dimer.

as small as 10 nM *(44, 45)* and sense gradients of over five orders of magnitude *(46, 47)*. The smallest detectable change (ΔS) in stimulus intensity increases with the background stimulus (S) to maintain a constant ΔS/S sensitivity rate, consistent with the Weber-Fechner Law *(48)*. The sensitivity ensures that a small stimulus triggers large changes in the direction of motor rotation. An inhibitory signal initiated by attractant binding can be amplified up to 35 times more than would be expected from the number of individual receptors that are inhibited *(44)*. This signal amplification has been shown to result mainly from modulation of CheA kinase by the receptors rather than changes in CheY-P affinity at the motor *(22)*. These results suggest that there must be functional interactions in stimulus detection and/or signal production of chemoreceptors.

The chemoreceptors, together with CheA and CheW, form higher-order structures called receptor patches *(49)*. These are typically found near the cell pole and contain all four MCPs and Aer *(50)*. In addition, at least some of the CheB, CheR, CheY, and CheZ molecules in the cell associate with these patches *(49, 51, 52)*, although none of these four proteins is required for patch formation.

The clustering of receptors almost certainly has a functional significance. As noted earlier, the crystal structure of the cytoplasmic domain of Tsr indicates that it exists as a trimer of dimers. Genetic evidence for the existence of such trimers is based on the disruptive effect of site-directed mutation of residues located at the dimer-dimer interface. Analysis of second-site suppressors of these mutations also indicated that the Tsr and Tar receptors co-mingle within the same trimer *(38)*.

In side view (Figure 1.4), CheW and CheA proteins are thought to bind at the distal

tip of the cytoplasmic domain of the receptor trimers. The bound CheA and CheW can form bridges that connect adjacent receptor trimers of dimers. A model for the interactions among receptors, CheW, and CheA within a receptor patch has been developed *(53)*. Bridges between receptor trimers consist of two CheW monomers and a CheA dimer. Each CheA subunit binds a CheW monomer, and CheW binds to the trimer of dimers at a dimer-dimer interface (Figure 1.5A). This basic structure can be extended into a hexagonal lattice of unlimited extent. This arrangement of receptors, CheW, and CheA would be conducive to cross-talk among receptors, either as members of mixed trimers of dimers or by communication within a linked population of receptor trimers. One can also imagine a dynamic situation in which connections among receptors are made and broken in response to ligand binding and/or covalent modification state. At least in part, CheA and CheW have different affinities to receptors in different signaling or methylation states *(54, 55)*. Therefore, stimulation of CheA kinase by the receptors can be controlled by modulating CheA and CheW binding to the receptors, potentially affecting the composition and arrangement of the receptor patch.

One possible function of clustering is to increase the sensitivity of the system by localizing all chemotaxis proteins in one large sensory complex. Each ternary receptor-CheW-CheA complex can be viewed as an allosteric enzyme that can be affected by ligand occupancy, covalent modification, and interaction among receptors. Being in a compact lattice could allow propagation of the signal received by one signaling complex throughout the cluster (Figure 1.5B). Also, a tight lattice organization of thousands of interacting chemoreceptor signaling complexes should promote inter-receptor

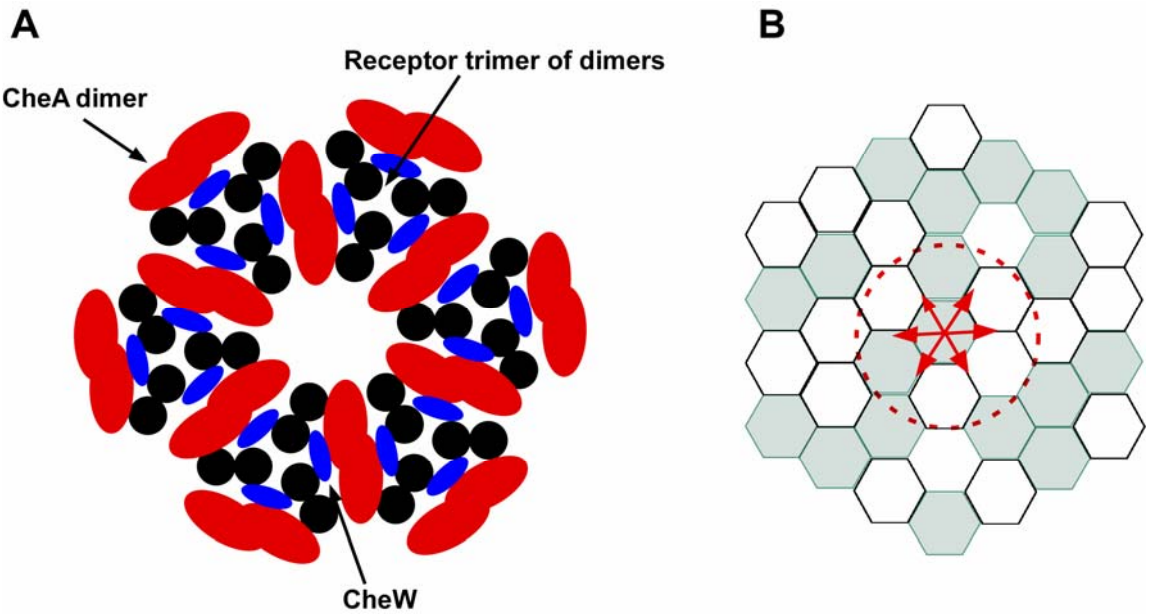

FIGURE 1.5 Higher-order receptor signaling complex (A) and a signal-propagation model (B). A schematic diagram (A) shows the hexagonal signaling complex formed by receptors bridged by CheA and CheW. Receptor monomers are shown as black circles that form trimers of homodimers. CheA dimers are shown as overlapped red ovals. The blue ovals represent CheW monomers. B, signaling network expanded from the hexagonal signaling complex in A with each hexagon representing a hexagonal complex. White and gray hexagons represents different trimers of dimers in different signaling states. A signal sensed by the center trimer of dimers could be propagated through the signaling network to neighboring complexes (red arrows and circle). The extent of the conformational spread is unknown.

communication.

SPECIFIC RESEARCH AIMS

Characterize functional interactions among different bacterial receptors. Much evidence suggests that bacterial receptors communicate extensively among themselves. It has become increasingly clear that a full comprehension of bacterial chemotaxis will require an understanding of how the component proteins function in the context of the receptor patches. That goal provides the impetus for the research described here.

I addressed several questions using *in vitro* biochemical assays and genetic methods. The most basic question is whether different receptors form mixed complexes with properties that transcend the sum of their component activities. For example, do receptors act synergistically to stimulate CheA, do they cooperate to inhibit CheA activity in response to attractant ligands, and do they engage in cross-talk? The four canonical chemoreceptors in *E. coli* share regions of strong sequence conservation, but there are marked differences in the behavior of isolated populations of the two high-abundance receptors (Tsr and Tar) and the two low-abundance receptors (Trg and Tap). Are some of the functional limitations of low-abundance receptors overcome when they interact with high-abundance receptors? Do low-abundance receptors alter properties of the high-abundance receptors?

Determine what roles the C-termini (last 50 residues) of high-abundance chemoreceptors play in chemotactic signaling. The extreme C-terminus of the high-abundance chemoreceptors is important for chemotactic signaling because the last five

residues (NWETF) of these proteins constitute a binding site for CheR methyltransferase and CheB methylesterase. In the absence of this sequence, the receptors remain undermethylated and are unable to adapt appropriately to attractant ligands. The low-abundance receptors naturally lack this NWETF motif and are, consequently, unable to maintain the appropriate level of methylation in the absence of high-abundance receptors. Adding the C-terminus of a high-abundance receptor onto a low-abundance receptor Trg can confer the ability to function independently of Tsr *(56)*. It has also been shown that some mutations that affect the C-termini of Tsr and Tar lock the receptors in their "on" (CheA kinase-stimulating) or "off" (CheA kinase-inhibiting) signaling modes. Some of these receptor mutations are dominant.

Based on these observations and our preliminary results, we think that the relatively unstructured C-terminal tail of the receptors and the C-terminus of CD2 do more than providing a docking site for CheR/CheB and a flexible tether for the NWETF sequence. I analyzed the function of receptors deleted for part or all of the C-terminus of Tar both *in vivo* and *in vitro*, and I also studied the effect of covalent modification on their behavior. My working hypothesis was that positively charged residues in this C-terminal region interact with the HAMP linker domain, the cell membrane, and/or the negatively charged glutamyl residues that constitute the methylation sites. I also used site-directed mutagenesis to assess the importance of these individual positively charged residues in signaling and adaptation.

CHAPTER II

COOPERATIVE SIGNALING AMONG BACTERIAL CHEMORECEPTORS*

SYNOPSIS

Four chemoreceptors in *Escherichia coli* mediate responses to chemicals in the environment. The receptors self-associate and localize to the cell poles. This aggregation implies that interactions among receptors are important parameters of signal processing during chemotaxis. We examined this phenomenon using a receptor-coupled in vitro assay of CheA kinase activity. The ability of homogeneous populations of the serine receptor Tsr and the aspartate receptor Tar to stimulate CheA was directly proportional to the ratio of the receptor to total protein in cell membranes up to a fraction of 50%. Membranes containing mixed populations of Tar and Tsr supported an up to 4-fold greater stimulation of CheA than expected on the basis of the contributions of the individual receptors. Peak activity was seen at a Tar:Tsr ratio of 4:1. This synergy was observed only when the two proteins were expressed simultaneously, suggesting that, under our conditions, the fundamental "cooperative receptor unit" is relatively static, even in the absence of CheA and CheW. Finally, we observed that inhibition of receptor-stimulated CheA activity by serine or aspartate required significantly higher

---

* Reproduced with permission from Lai, R. Z., Manson, J. M., Bormans, A. F., Draheim, R. R., Nguyen, N. T., and Manson, M. D. (2005) Cooperative Signaling among Bacterial Chemoreceptors, *Biochemistry 44*, 14298-307. Copyright 2005 American Chemical Society

concentrations of ligand for membranes containing mixed Tsr and Tar populations than for membranes containing only Tsr (up to 10^2-fold more serine) or Tar (up to 10^4-fold more aspartate). Together with recent analyses of the interactions of Tsr and Tar in vivo, our results reveal the emergent properties of mixed receptor populations and emphasize their importance in the integrated signal processing that underlies bacterial chemotaxis.

INTRODUCTION

Motile bacteria migrate toward or away from certain chemicals in a behavior called chemotaxis (reviewed in refs. *(57-60)*). In *Escherichia coli*, these chemicals are recognized by one of four closely related chemoreceptors that localize to the cell membrane. The Tar receptor mediates attractant responses to L-aspartate and maltose, as Tsr does to L-serine. Trg mediates responses to ribose, glucose, and galactose, and Tap is responsible for chemotaxis toward di- and tripeptides. The coupling factor CheW connects the histidine-protein kinase CheA to the membrane-distal tip of the cytoplasmic domain of these receptors *(61)*. Occupancy of ligand- binding sites in the periplasmic domain of the receptors modulates the autophosphorylation activity of CheA. Phosphorylated CheA, in turn, transfers its phosphoryl group to the response regulator CheY. Binding of phospho-CheY to FliM in the flagellar motor increases the probability of a reversal from counterclockwise (CCW) rotation of the flagellum to clockwise (CW). The balance between the activities of CheA and the CheY phosphatase, CheZ, determines the CCW to CW ratio of flagellar rotation. CCW rotation leads to smooth swimming, and CW rotation of one or more flagella induces a tumble.

CheA activity is also modulated by the methylation state of the receptor to which it is coupled. Methyl groups are added by a methyltransferase, CheR, and removed by a methylesterase, CheB. CheB is much more active when it is phosphorylated by CheA. Increased levels of methylation at four specific glutamyl residues bias a receptor toward CheA stimulation, whereas decreased levels of methylation cause a receptor to be less active in stimulating CheA. Adjustments in the relative rates of methylation and demethylation allow the receptor ensemble to maintain nearly the same baseline level of CheA activity at any constant concentration of attractant or repellent. Tar and Tsr are both synthesized with the first and third methylatable glutamyl residues as glutaminyl residues to produce the QEQE form of the receptors, in which Q functionally mimics methylated glutamyl residue (E^m). Phospho-CheB then deamidates these two glutaminyl residues to generate the EEEE form of the receptors. All of the in vitro studies described here were performed with the QEQE forms of Tar and Tsr.

E. coli chemoreceptors localize to cell poles *(49)* in clusters that contain all four receptors *(50)*. Formation of these clusters requires CheW and CheA. In addition, at least some of the CheB, CheR, CheY and CheZ proteins in the cell are associated with these patches *(49, 51, 52)*, although none of them are required for patch formation or maintenance. Receptor clustering has also been observed in other bacteria *(62, 63)*.

The crystal structure of the cytoplasmic domain of the Tsr receptor indicates that it, and presumably the other receptors, exists as a trimer of dimers *(35)*. Genetic studies also provide evidence for the existence of such trimers *(36)*. It has been proposed that arrays of such trimers of dimers connected by CheW and CheA can form higher order

lattices within a patch *(53, 64)*.

Close physical association of receptors suggests that they interact in chemotaxis signaling. *E. coli* can detect sub-micromolar concentrations of some attractants *(65)*, and gradients can be sensed over five orders of magnitude *(46, 47)*. Also, the inhibitory signal initiated by ligand binding can be amplified up to 35 times more than expected from shutting off individual receptors *(44)*. Thus, it seems crucial to consider the activity of the chemoreceptor patch as a whole *(53, 66-70)* and to take relatively long-range interactions among receptors into account *(36, 71, 72)*.

We report here the results from in vitro receptor-coupled kinase assays designed to examine such higher-order interactions. We find that the receptors Tar and Tsr combine synergistically to stimulate CheA to levels unattainable by either receptor in isolation. Mixed receptor populations also show decreases of several orders of magnitude in their sensitivities to aspartate and serine. Finally, we present evidence that the interactions among receptors that lead to these phenomena are stable for hours, both within cells and in inner-membrane preparations.

MATERIALS AND METHODS

Bacterial strains and plasmids. E. coli strain RP3098 [Δ*(flhD-flhB)*4] *(73)*, a derivative of *E. coli* K12 strain RP437 *(74)*, was used for high-level expression of chemoreceptors and CheA. Strain BL21(λDE3) (Novagen) was used to produce CheY for purification. The λDE3 derivative of BL21 [F^- *ompT* $hsdS_B$ $(r_B^- m_B^-)$ *gal dcm*] contains a prophage that encodes the T7 RNA polymerase gene under the control of the *lacUV5*

promoter *(75, 76)*.

Plasmid pDM011 is a pET24a(+) derivative containing *cheY* gene expressed from a T7 promoter. Plasmid pKJ9 carries an isopropyl-D-thiogalactopyranoside (IPTG)-inducible *cheA* gene *(77)*. Plasmid pCJ30, a derivative of the ColE1 plasmid pBR322, confers Amp^r and carries a *tac* (IPTG-inducible) promoter preceding a multiple cloning site *(6)*. Plasmid pBAD18, also a derivative of pBR322, confers Amp^r and has the *araBAD* promoter preceding a multiple cloning site *(78)*. Plasmid pLC112, a derivative of the P15A plasmid pACYC, confers Cam^r and has the *nahG* (salicylate-inducible) promoter preceding a multiple cloning site *(36)*. Plasmid pBAL03 was constructed from pACYC and pBAD18. It bears the P15A origin, confers Cam^r, and has the *araBAD* promoter preceding a multiple cloning site. The wild-type *tar* and *tsr* genes were introduced into these plasmids to allow control of their expression by different inducers and, in the case of the *araBAD* promoter, for repression by the addition of the anti-inducer fucose *(78-80)*. Table 2.1 provides a complete list of strains and plasmids used in this study.

Purification of CheY and CheA. CheY was purified according to Matsumura et al. *(81)*, with minor modifications. Transcription of *cheY* was induced from plasmid pDM011 by with 500 μM IPTG in a 1-L Luria Broth (LB) *(82)* culture of strain BL21 (λDE3) grown at 30°C. CheY was eluted from a Cibacron blue column, dialysed, and then concentrated by ultrafiltration before loading onto a Superose 12 column. CheA was purified by the method of Hess and Simon *(83)*. CheA expression from the pKJ9 plasmid in strain RP3098 was induced at 30°C by adding IPTG to a final concentration

Table 2.1. Bacterial strains and plasmids used in this study

Strain or plasmid		Genotype	Comments	Reference or source
Strain				
	RP437	*thr-1*(Am) *leuB6 his-4 metF159*(Am) *eda-50 rpsL1356 thi-1 ara-14 mtl-1 xyl-5 tonA31 tsx-78 lacY1* F^-		(27)
	RP3098	RP437 Δ*(flhD-flhB)*4		(26)
	BL21 (λDE3)	BL21 *ompT* $hsdS_B$ ($r_B^- m_B^-$) *gal dcm* F^-		(28,29)
Plasmid				
	pDM011	*pT7 CheY* Kan^r	Expresses CheY	Philip Matsumura
	pKJ9	*ptac CheA* Ampr	Expresses CheA	(30)
	pCJ30	*ptac* $lacI^q$ Amp^r	*ptac* expression vector	(31)
	pBAD18	*paraBAD* $araC^+$ Amp^r ColE1 origin	p*araBAD* expression vector	(32)
	pLC112	*pnahG* $nahR^+$ Cam^r P15A origin	*pnahG* expression vector	(13)
	pBAL03	*paraBAD* $araC^+$ Cam^r P15A origin	p*araBAD* low expression vector	This study

of 500 μM to a 1-L LB culture. The purities of CheY and CheA were estimated from densitometric scans (ImageMax scanner) of Coomassie blue-stained 16% or 12% acrylamide SDS gels, respectively. Total protein concentration was determined using the Bradford assay *(84)*.

Preparation of inner membranes containing overexpressed receptors. Cultures were grown in 1 L of LB broth at 30°C. Receptor synthesis from plasmid-borne *tar* and *tsr* genes was induced in strain RP3098 by addition of the desired concentration of the relevant inducer at the appropriate time. Cells were harvested at OD_{600} ~ 1.0 by centrifugation at 4,500 x g, using a Beckman JA10 rotor.

The preparation of inner membranes was based on the method of Osborn and Munson *(85)*. Spheroplasts were made from the harvested cells and lysed by osmotic shock. Cell debris was removed by centrifugation at 1,200 x g. Membranes were pelleted at 17,700 x g, washed, and resuspended in a 25% (w/v) sucrose solution. Membranes were fractionated on a sucrose step gradient (4 ml 55% sucrose, 8 ml 45% sucrose, 8 ml 40% sucrose, and 10 ml 30% sucrose [w/v]) in a Beckman SW28 rotor operated at 4°C and 140,000 x g for 12 h. The band at the interface of the 30% and 40% sucrose layers contained the highest percentage of receptor to total protein. This fraction was dialyzed twice against 2 L TE buffer (10 mM Tris, 1 mM EDTA, pH 8.0), then pelleted by centrifugation at 210,000 × g and resuspended in TE buffer containing 15% glycerol (v/v). The ratio of receptor to total protein was determined by quantitative scanning-densitometry of Coomassie-stained 12% SDS gels using the ImageMax scanner and NIH imager software. The total protein concentration was determined by the Bradford assay

(84).

In vitro receptor-coupled phosphorylation assay. The receptor-coupled phosphorylation assay was performed using a modified version of the procedure of Borkovich and Simon *(86)*. Five pmol CheA and 20 pmol CheW were mixed and incubated at 4ºC overnight in a total volume of 2.5 µL to maximize formation of CheW:CheA dimer:CheW complexes. Then, 500 pmol CheY, 0.5 µL 20X phosphorylation buffer (1 M Tris-HCl, 1 M KCl, 100 mM $MgCl_2$, pH 7.5), 0.5 µL 40 mM DTT, and an aliquot of an inner-membrane preparation containing 20 pmol receptor were added to the CheA and CheW mix to yield a total volume of 8 µL. For assays involving chemoeffectors, 1 µL of a solution containing ligand at the desired concentration was added. The mixtures were incubated for 4 h at room temperature to allow ternary complexes of receptor/CheA/CheW to assemble. Reactions were initiated by addition of 1 µL [γ-32P]-ATP (a mixture of 3.3 µM radioactive ATP with 10 mM unlabeled ATP at a 1:1 ratio). Reactions were halted after 20 s by the addition of 40 µL 2x SDS-PAGE sample buffer, and samples were subjected to 16.5% acrylamide SDS-PAGE. Gels were dried and analyzed using a phosphorimager (Fuji BAS 2000). Phospho-CheY levels were calibrated with reference to densitometric scans of a dilution series of [γ-^{32}P]-ATP spots made with the same batch of [γ-^{32}P]-ATP used in the assay from that day.

The effect of *E. coli* membrane per se on the *in vitro* CheA activity was tested in parallel assays in the presence of: (A) no added membranes; (B) receptor-free membranes; (C) receptor-containing membranes; and (D) mixtures of receptor-

containing and receptor-free membranes. No significant difference in CheA activity was seen between assays A and B, and, for an equal concentration of receptor, the same large increase in CheA activity was observed in assays C and D (data not shown).

Data analysis. Ligand-dependent inhibition of receptor-coupled CheA kinase activity was analyzed as described previously *(87)*. The titration curves were fitted with the Hill equation, using KaleidaGraph v3.6 software. The analysis yielded two parameters: the half-maximal inhibitory concentration (IC_{50}) and the Hill coefficient for binding cooperativity, n_H. Standard deviations of the mean for the IC_{50} and n_H values were calculated, with $n \geq 3$.

The distribution of CheA kinase activity stimulated by simultaneously expressed Tar and Tsr was fitted with a Beta Distribution, Beta(a,b) *(88)*, using MATLAB v7.0 software. The Beta distribution is designed to fit a set of bounded (between 0 and 1) data. Because the CheA activity stimulated by Tsr is twice that of Tar, the left endpoint is lower than the right endpoint. Thus, a background activity corresponding to the expected contribution of Tsr and Tar, assuming they do not interact synergistically, was subtracted from the CheA activities actually measured at each Tar/Tsr ratio examined. The transformed data were then fitted with the Beta function. Finally, the background values were added back to yield the curve shown. The symmetry properties of the distribution were determined from the skew of the fitting curve.

Receptor-activity simulation program. In our model of receptor interactions we made the simplifying assumption that the functional unit is a trimer of dimers. Although we do not now think that this molecular structure is preserved in ternary

receptor/CheA/CheW complexes, we propose that receptors are delivered to the functional signaling assemblages as trimers of dimers. Thus, the association of receptors in trimers of dimers will be a major factor in determining the nearest neighbors of a receptor dimer within the actual signaling array. This controversial point is examined in detail in the Discussion.

Our receptor-activity simulation program (Program 1S in Supplementary Material of reference *(89)*) uses a Monte Carlo approach to find the distribution of trimers of dimers of Tsr and Tar. A full description of the program is provided in the Supplementary Materials. Each dimer is considered to be a homogenous receptor unit. There are four trimer types, and the probability of formation for each is stored in a table. The user can specify the number of each type of receptor homodimer in the population. The program chooses a random sample of three receptor dimers from the population. If they form trimers as specified by the probability table, they are removed from the uncombined dimer population. This selection and combination process continues until there are no uncombined receptors left. The calculated distribution of receptor trimers is then written to a file for the user to analyze. Any value of CheA-stimulating activity for a given trimer type (Tar/Tar/Tar, Tar/Tar/Tsr, Tar/Tsr/Tsr, and Tsr/Tsr/Tsr) can be assigned. We assigned the same total activity to the two mixed trimers, since each contains an equal number of Tar/Tsr and Tsr/Tar dimer interfaces.

RESULTS

Dependence of CheA activity on receptors as a fraction of total membrane protein.

Before we could evaluate interactions among different receptors, we first had to determine the interactions among receptors of one type. To examine how the receptor fraction of total membrane protein affects the ability of Tar and Tsr to stimulate CheA kinase activity, inner membranes were prepared in which receptors made up 3% to 75% of the total protein. An equal total amount (20 pmol) of receptor was used in each assay. Both Tar and Tsr showed a striking increase in the ability to stimulate CheA with increasing receptor fraction (Figure 2.1). The linear fits of the data obtained with each receptor were done separately for activities measured at receptor levels ≤ 50% of total protein and ≥ 50% of total protein because there was an obvious discontinuity at this point. There was considerably more scatter in the Tsr data. Equations 2.1 to 2.4 define the lines obtained,

$$\nu_{Tar} = 0.062 \times P_a + 0.7 \quad P_a \leq 50 \tag{2.1}$$

$$\nu_{Tar}' = 0.002 \times P_a + 3.8 \quad P_a \geq 50 \tag{2.2}$$

$$\nu_{Tsr} = 0.133 \times P_s + 0.5 \quad P_s \leq 50 \tag{2.3}$$

$$\nu_{Tsr}' = 0.024 \times P_a + 5.7 \quad P_s \geq 50 \tag{2.4}$$

where ν_{Tar} and ν_{Tsr} represent CheA kinase activity supported by Tar and Tsr, respectively, expressed as pmol phospho-CheY produced per sec, and P_a and P_s represent Tar and Tsr, respectively, as a proportion of total protein.

The lines for Tar and Tsr ($P \leq 50$) intercept the ordinate at about 0.7 and 0.5 pmol phospho-CheY·s^{-1}, respectively. For comparison, the CheA activity in the absence of receptor is ~ 0.1 pmol phospho-CheY·s^{-1} under our assay conditions. This extrapolation

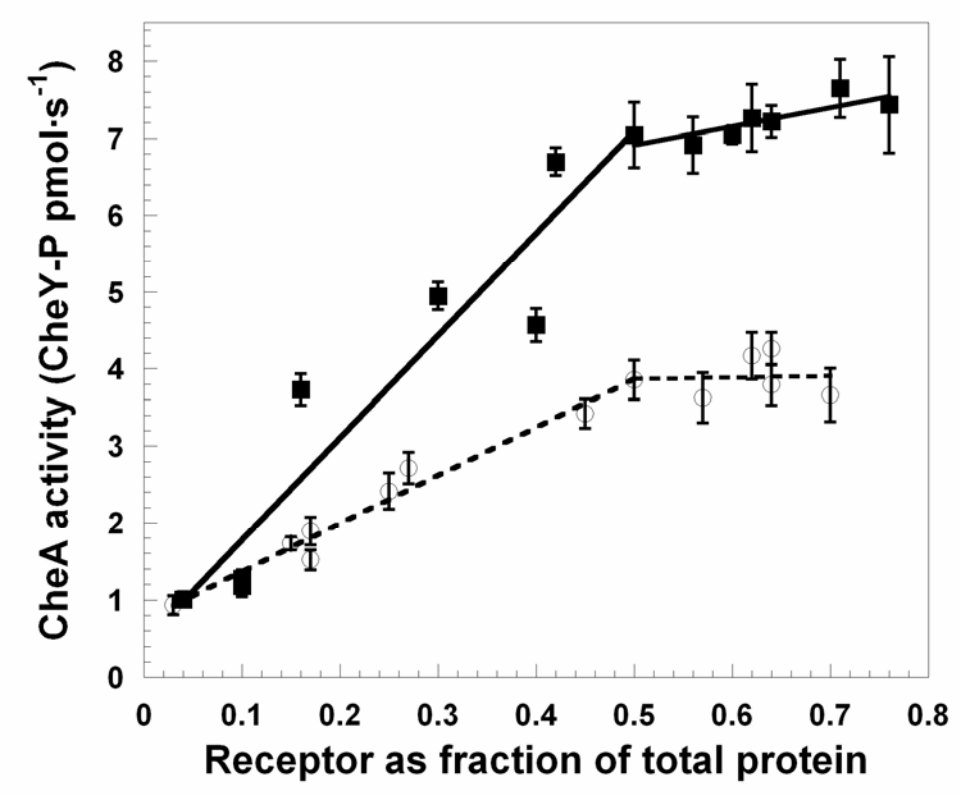

FIGURE 2.1 Effect of receptor as a fraction of total membrane protein on CheA activity. CheA activity stimulated by receptors expressed at different levels was determined using the in vitro receptor-coupled CheY-phosphorylation assay. CheA activity is expressed as the amount of phospho-CheY produced per second normalized to 1 percent receptor. The total amount of receptor present was the same in each assay. The fraction of receptor to total protein was measured as described in Materials and Methods. The data for Tar and Tsr are shown as open circles and closed squares, respectively. Each point is the mean value from three independent measurements with a given receptor preparation. The error bars show the standard deviation of the mean, with n = 3.

suggests that, even at extreme dilution in the membrane, receptors can stimulate CheA activity by about five fold. The two-fold steeper slope of the Tsr line for receptor levels of ≤ 50% of total protein is consistent with reports in the literature *(61, 90)* and the results of this study that Tsr is about twice as effective as Tar at stimulating CheA.

Since receptor activities depended strongly on their expression level, it seemed possible that the range over which CheA stimulation would increase linearly with total receptor amount might vary at different receptor expression levels. This possibility was tested by determining CheA activity as a function of receptor concentration with membrane preparations in which Tar or Tsr was present as a different fraction of total protein. CheA activity increased linearly with Tar or Tsr concentration up to 80 pmol/20 μL of reaction mix with all preparations tested (Figure 2.2). We accordingly selected 20 pmol receptor per reaction, which is well within the linear range, as our standard assay condition.

Tar and Tsr expressed in separate cells do not interact in mixed membrane preparations. Membrane preparations containing Tar or Tsr at 27% and 30% of total protein, respectively, were mixed at ratios of 2:1, 1:1, and 1:2 while holding the total amount of receptor constant at 20 pmol. These samples were then subjected to the in vitro receptor-coupled CheA assay. The activity supported by the mixed receptor populations was within ±16% of the sum of the activities expected for the individual receptors assayed separately (Table 2.2). It should be noted that we do not know whether our membranes fuse under the conditions of our assay, but the results obtained suggest that, if they do, the fusion has no functional consequence.

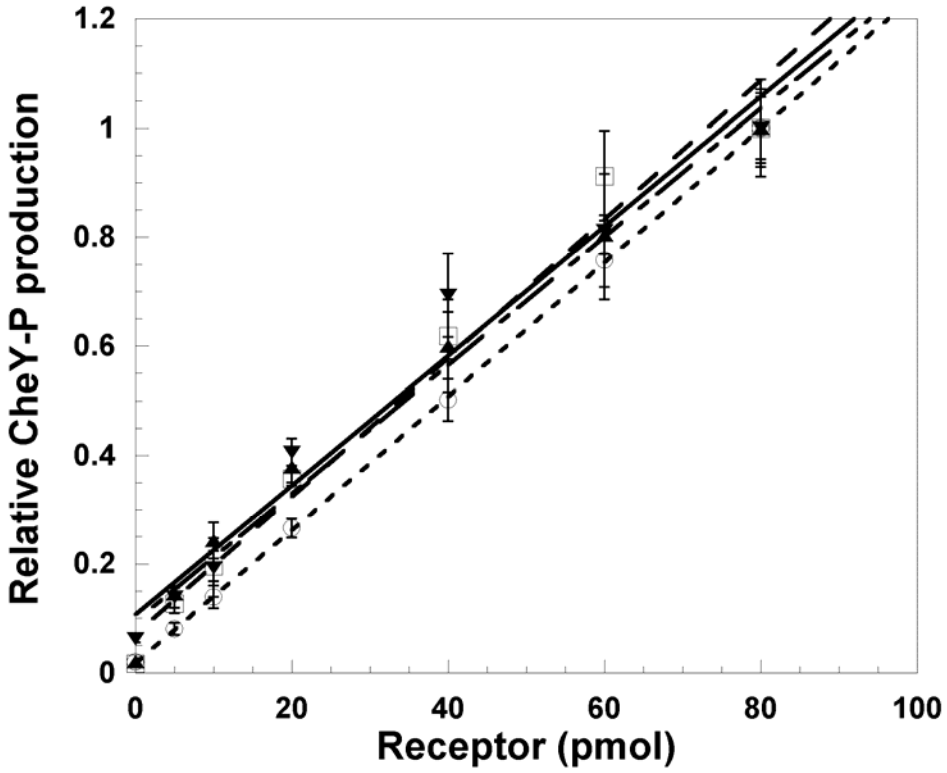

FIGURE 2.2 CheA activity as a function of total receptor amount. Receptor-stimulated CheA kinase activity at different receptor expression levels was determined as a function of total receptor amount using the in vitro phosphorylation assay. CheA, CheW, and CheY were held constant, as was the total reaction volume. Tar (10% of total membrane protein), open squares, dashed line; Tar (42% of total membrane protein), open circles, dotted line; Tsr (10% of total membrane protein), upside-down triangles, solid line; and Tsr (45% of total membrane protein), rightside-up triangles, line with alternating short and long dashes.

Table 2.2 CheA activity stimulated by mixtures of Tar-containing and Tsr-containing membranes[a]

Tar:Tsr ratio	CheA activity (pmol CheY-P·s^{-1})		
	Tar membranes alone	Tsr membranes alone	Mixed membranes
1:2	0.9 ± 0.2	3.3 ± 0.6	4.4 ± 0.7
1:1	1.4 ± 0.2	2.5 ± 0.2	3.3 ± 0.4
2:1	1.8 ± 0.3	1.6 ± 0.3	2.9 ± 0.4

[a] The fractions of receptor to total protein were 27% and 30% for Tar-containing and Tsr-containing membranes, respectively. The same volumes of membrane preparations used to assay the CheA activities supported by individual receptors were combined for the assays of mixed membranes.

Sequentially co-expressed Tar and Tsr do not interact. E. coli chemoreceptors localize to the cell poles in the absence of CheA and CheW, although they do not form tight clusters. Thus, the overall dynamics of receptor interactions in the presence and absence of CheA and CheW are still not clear, although they have been the subject of intensive investigation *(36, 39, 49, 71)*. To investigate the stability of receptor interactions under our admittedly non-physiological conditions of overexpression, we produced Tar and Tsr sequentially in the same cells. Synthesis of one receptor was induced for 2 to 3 h with 0.2% arabinose from a plasmid in which the gene was transcribed from the *araBAD* promoter control. Then, 0.4% fucose was added to block all subsequent expression of that receptor (*33-35*). After 10 min, synthesis of the second receptor was induced with IPTG or salicylate, as appropriate, and the cells were allowed to grow for another 2 to 3 h, for a total of 5 h. The membranes prepared from these cells were designated Tar//Tsr if Tar was expressed first and Tsr//Tar if Tsr was expressed first. The results of receptor-coupled CheA kinase assays conducted with these membranes are shown in Figure 2.3.

As in the experiments carried out with the mixed membrane preparations, interpretation of these results requires an estimate of the activities expected if there is no functional interaction among the receptors. Because of the strong dependence of receptor-stimulated CheA activity on the fraction of Tar and Tsr in the membrane, we set up two boundary conditions. The lower one assumed that Tar and Tsr do not interact in any way, so that the baseline activity for each receptor can be estimated from the fraction of that receptor only. On this basis, the total activity of the mixed population is

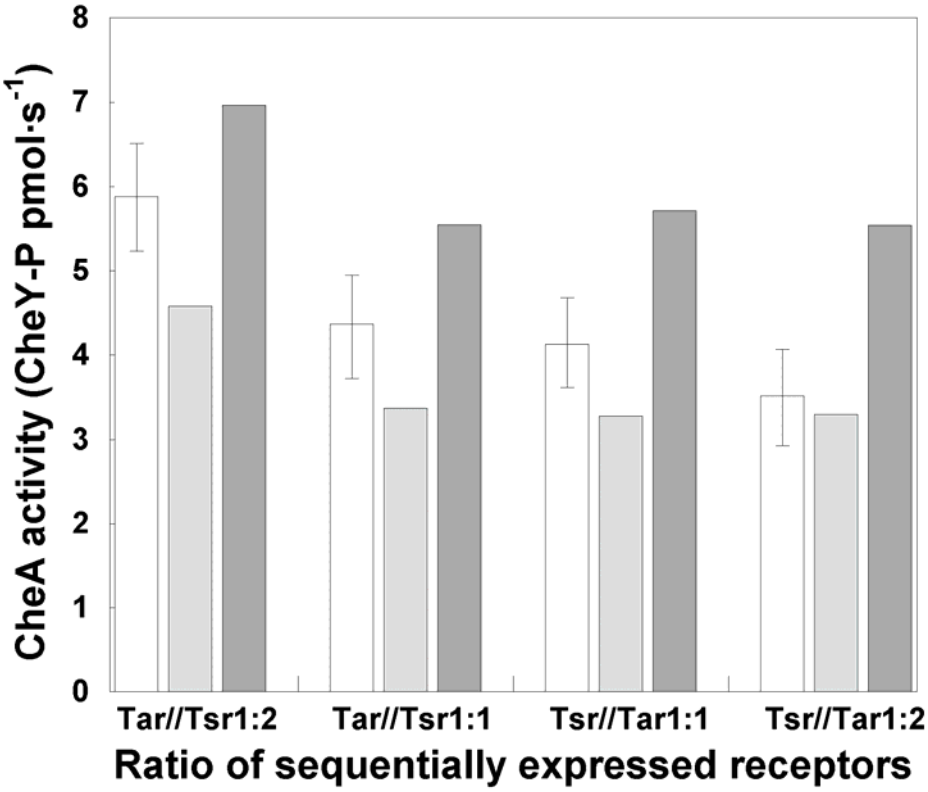

FIGURE 2.3 CheA-stimulating activity of membranes containing Tar and Tsr expressed sequentially in the same cells. CheA kinase activities stimulated by Tar//Tsr and Tsr//Tar membranes (see text for definitions) at different ratios of the receptors (indicated below the histogram) are shown as white bars. Values of ν_L (gray bars) and ν_H (black bars) were calculated from Equation 5 and Equation 6 or 7, respectively. The fractions of receptor relative to total protein were 72.4% for Tar//Tsr 1:2 ratio, 61.5% for Tar//Tsr 1:1 ratio, 59.9% for Tsr//Tar 1:1 ratio, and 68.2% for Tsr//Tar 1:2 ratio.

given by Equation 2.5,

$$\nu_L = [(0.062 \times P_a + 0.7)P_a + (0.133 \times P_s + 0.5)P_s]/(P_a + P_s) \quad \{P_a \leq 50 \text{ and } P_s \leq 50\} \tag{2.5}$$

where ν_L is the activity expected if there is no functional interaction, and P_a and P_s have the same meanings as in Equations 1 to 4. The upper boundary assumes that the total receptor fraction should be used to calculate the activity expected from each receptor. The activity of the mixed population is then given by Equation 2.6 (for fractions ≤ 50%) or Equation 2.7 (for fractions ≥ 50%),

$$\nu_H = \{[0.062 \times (P_a+P_s) + 0.7]P_a + [0.133 \times (P_a+P_s) + 0.5]P_s\}/(P_a + P_s) \quad \{P_a + P_s \leq 50\} \tag{2.6}$$

$$\nu_H = \{[0.002 \times (P_a+P_s) + 3.8]P_a + [0.024 \times (P_a+P_s) + 5.7]P_s\}/(P_a + P_s) \quad \{P_a + P_s \geq 50\} \tag{2.7}$$

where ν_H is the activity expected if the fractions of the two receptors are combined to calculate the receptor fraction used to determine the contribution of each receptor to overall activity.

The values of ν_L and ν_H set the lower and upper limits for the receptor-coupled CheA activity expected if there is no positive or negative cooperativity between Tar and Tsr. As seen in Figure 2.3, the CheA activities supported by the Tar//Tsr and Tsr//Tar membranes fall between the values of ν_L and ν_H for each preparation. We conclude that there is no significant functional interaction between Tar and Tsr when they are

expressed sequentially in the same cells.

Tar and Tsr expressed simultaneously interact synergistically. The results described in the previous paragraphs demonstrate that receptors overexpressed separately, in time or space, in the absence of CheA and CheW do not interact functionally when CheA and CheW are subsequently added. We wanted to extend our analysis to ask whether Tar and Tsr exhibit different behavior in mixed populations when they are synthesized, and presumably inserted into the membrane, at the same time. To this end, membranes were prepared from cells in which Tar and Tsr were expressed together at different ratios.

Tar and Tsr, encoded by compatible plasmids, were induced together in cultures that had reached an OD_{600nm} of 0.1. The IPTG concentrations used were chosen based on which gene was under control of the *tac* promoter. This approach is valid because RP3098 is a *lacY* strain in which the level of induction is proportional to the concentration of IPTG over a fairly wide range. Synthesis of the other receptor was induced with a saturating concentration of its inducer, either salicylate or arabinose.

Membranes were prepared from these cells and used in the in vitro CheA assay. All the samples were normalized to the CheA kinase activity contributed by one percent of receptor to total protein in order to correct for the large effect of receptor fraction on activity. The normalized activities measured with membranes in which Tar and Tsr were simultaneously expressed were all significantly higher than the ν_H values (Figure 2.4). The data set was fit with a Beta distribution (a = 2, b = 4). The curve is skewed toward the Tar side, with a peak when the Tsr/(Tar + Tsr) ratio is about 0.2. The activities for

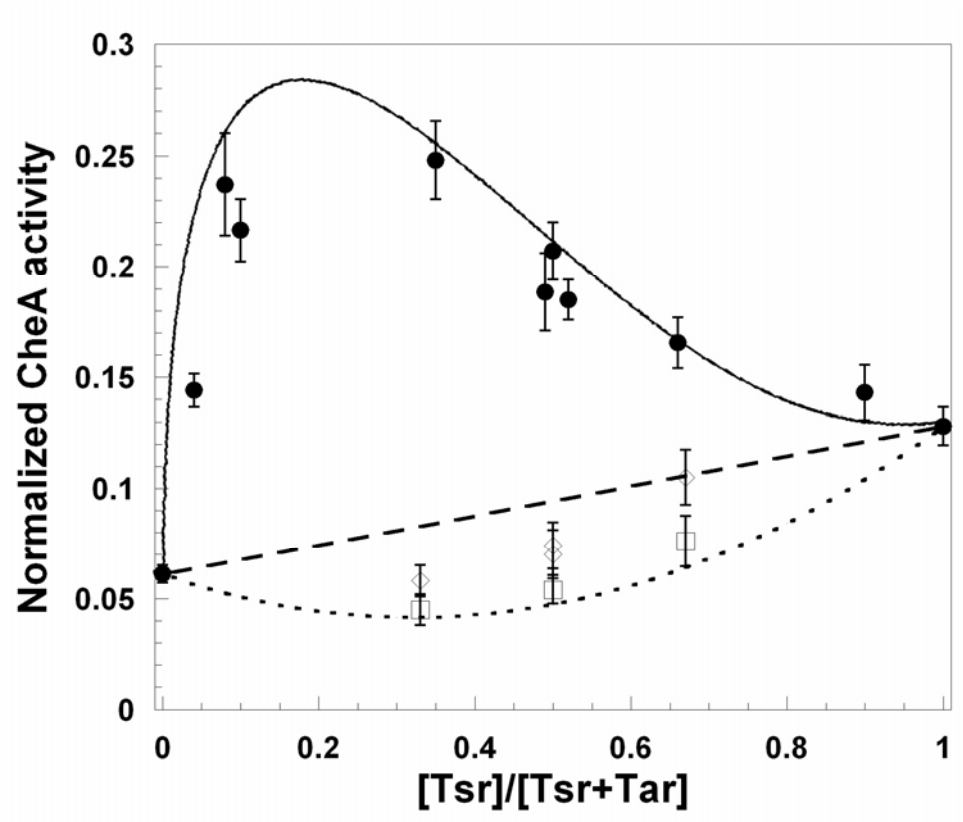

FIGURE 2.4 Co-expressed Tar and Tsr interact synergistically to stimulate CheA. CheA kinase activities (closed circles) stimulated by membranes containing Tar and Tsr co-expressed at the ratios indicated were measured in the *in vitro* receptor-coupled CheA kinase assay. Values of ν_L (dotted line) and ν_H (dashed line) were calculated using Equation 5 and Equation 6 or 7, respectively. Data for mixed Tar + Tsr membranes (open squares) from Table 2.1, and data for membranes containing sequentially expressed receptors (open diamonds) from Figure 2.3, are included for comparison. CheA activity was normalized to the average contribution of each receptor in the reaction.

mixed Tsr-containing and Tar-containing membranes or membranes from cells in which Tsr and Tar were expressed sequentially all fell between the calculated values for ν_L and ν_H and are shown for comparison.

Receptor stoichiometry affects the response to attractants. Another measure of the functional interaction between receptors is how their CheA-stimulating activities are inhibited by attractant ligands. When Tar and Tsr are expressed together, each should stimulate some fraction of CheA activity, and the Tar or Tsr portion of the activity should be inhibited by the addition of aspartate or serine, respectively. Titration of receptor-coupled CheA activity with these attractants is shown in Figure 2.5. For simultaneously expressed, mixed receptor populations, neither serine nor aspartate inhibited CheA activity entirely. Therefore, maximum inhibition by an attractant was defined by the activity corresponding to the plateau value reached at the highest concentrations of that attractant. The titration curves were fitted with the Hill equation *(87)*, which yielded two parameters: a half-maximum inhibitory concentration, IC_{50}, and a binding-cooperativity Hill coefficient, n_H. The IC_{50} and n_H values for both serine and aspartate were significantly different for membranes containing mixed receptor populations than for membranes containing Tar or Tsr alone (Table 2.3). The IC_{50} for serine increased from 2.6 x 10^{-4} M to about 3 x 10^{-2} M (~ 10^2 fold), and the corresponding change with aspartate was from 7.6 x 10^{-6} M to more than 6 x 10^{-2} M (~ 10^4 fold). The values of n_H decreased from about 2 to about 1. Neither of these effects was seen with mixtures of Tar-containing and Tsr-containing membranes or with membranes containing sequentially expressed Tar and Tsr (Table 2.3).

FIGURE 2.5 Effect of receptor stoichiometry on attractant-mediated inhibition of receptor-coupled CheA kinase. CheA activity was measured in the in vitro receptor-coupled assay. Normalized CheA activity was determined for a series of aspartate (A) and serine (B) concentrations. A best-fit curve was calculated using the Hill equation. The different mixtures are indicated as follows: Tar only, open circles; Tsr only, open squares; Tar:Tsr (10:1) filled circles, Tar:Tsr (2:1), filled inverted triangles; Tar:Tsr (1:1), filled squares; Tar:Tsr (1:2), filled upright triangles; Tar:Tsr (1:10), filled diamonds. Note that inhibition of heterologous receptors (Tsr by aspartate and Tar by serine) may obscure the expected plateau for the inhibition of cognate receptors (Tar by aspartate and Tsr by serine) at the highest concentrations of attractants.

A

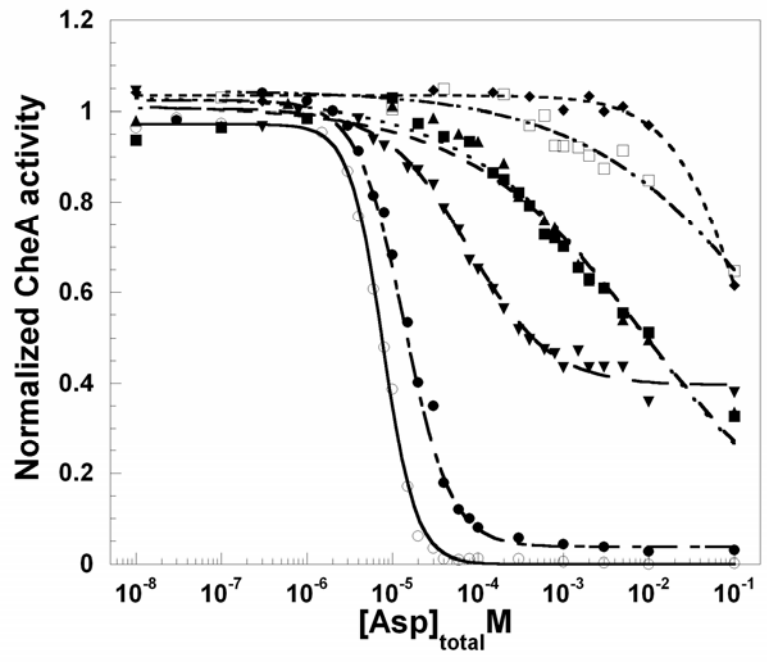
Normalized CheA activity
1.2
1
0.8
0.6
0.4
0.2
0
10^{-8} 10^{-7} 10^{-6} 10^{-5} 10^{-4} 10^{-3} 10^{-2} 10^{-1}
$[Asp]_{total}$M

B

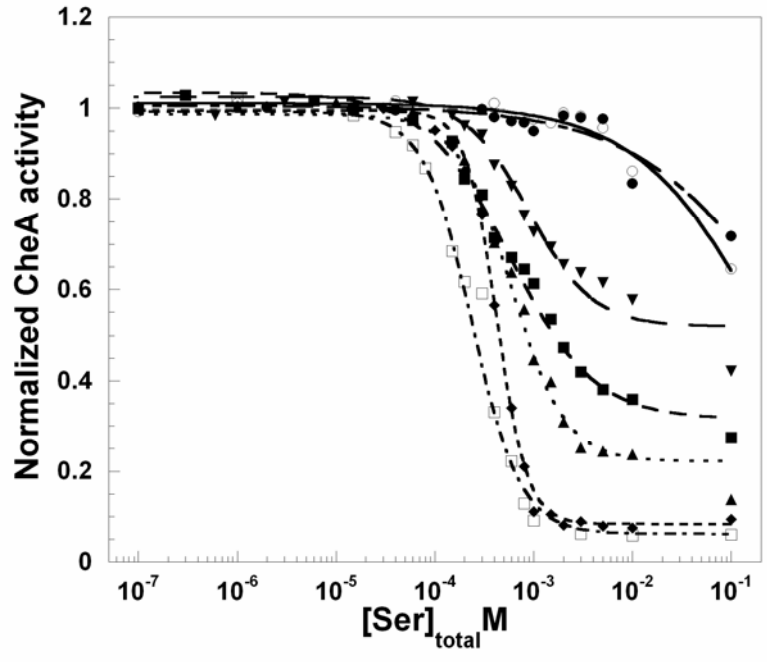
Normalized CheA activity
1.2
1
0.8
0.6
0.4
0.2
0
10^{-7} 10^{-6} 10^{-5} 10^{-4} 10^{-3} 10^{-2} 10^{-1}
$[Ser]_{total}$M

Table 2.3 Ligand-inhibition parameters estimated from the Hill equation

[Tsr]/[Tar+Tsr]	%Tar[a]	%Tsr[a]	ν_{max}[b]	ν_{min}[c] for Ser	ν_{min}[c] for Asp	IC_{50} for Ser (μM)	n_H	IC_{50} for Asp (μM)	n_H
1.0	0	30	0.13 ± 0.01	0.01 ± 0.004	0.08 ± 0.01	260 ± 13	1.8 ± 0.1	≥ 9000	*n/a*[g]
0.92	2.8	32	0.14 ± 0.01	0.02 ± 0.01	0.05 ± 0.01	540 ± 28	2.4 ± 0.2	≥ 60000	*n/a*[g]
0.90	2.8	26	0.15 ± 0.02	0.01 ± 0.003	0.09 ± 0.02	420 ± 18	2.9 ± 0.3	$\geq 1.4\times10^5$	*n/a*[g]
0.89	3.2	26	0.15 ± 0.01	0.02 ± 0.003	0.06 ± 0.01	370 ± 20	2.3 ± 0.2	$\geq 7\times10^5$	*n/a*[g]
0.67	15	30	0.17 ± 0.01	0.02 ± 0.01	0.06 ± 0.02	730 ± 35	1.3 ± 0.1	1400 ± 100	0.7 ± 0.1
0.52	29	31	0.21 ± 0.01	0.04 ± 0.02	0.07 ± 0.02	800 ± 95	0.9 ± 0.1	1500 ± 330	0.9 ± 0.2
0.49	29	28	0.19 ± 0.02	0.05 ± 0.01	0.06 ± 0.01	760 ± 49	1.0 ± 0.1	760 ± 48	1.0 ± 0.1
0.35	35	19	0.25 ± 0.02	0.1 ± 0.03	0.09 ± 0.03	1500 ± 133	0.9 ± 0.1	75 ± 6	0.8 ± 0.04
0.10	20	2.2	0.22 ± 0.02	0.12 ± 0.02	0.01 ± 0.003	≥ 30000	*n/a*[g]	17.2 ± 0.7	1.9 ± 0.1
0.082	20	1.8	0.24 ± 0.02	0.15 ± 0.01	0.01 ± 0.002	≥ 20000	*n/a*[g]	15.4 ± 0.7	1.6 ± 0.1
0.037	21	0.8	0.14 ± 0.01	0.09 ± 0.02	0.01 ± 0.01	≥ 20000	*n/a*[g]	10.8 ± 0.4	1.7 ± 0.1
0	25	0	0.06 ± 0.004	0.04 ± 0.01	0	≥ 14000	*n/a*[g]	7.6 ± 0.3	2.1 ± 0.1

Table 2.3 Continued

[Tsr]/[Tar+Tsr]	%Tar[a]	%Tsr[a]	ν_{max}[b]	ν_{min}[c] for Ser	ν_{min}[c] for Asp	IC_{50} for Ser (μM)	n_H	IC_{50} for Asp (μM)	n_H
0.53[d]	27	30	0.05 ± 0.01	0.01 ± 0.003	0.03 ± 0.01	270 ± 20	2.1 ± 0.3	8.0 ± 0.5	2.0 ± 0.4
0.53[e]	29	32	0.07 ± 0.01	0.02 ± 0.01	0.04 ± 0.01	280 ± 25	1.7 ± 0.3	8.2 ± 0.4	2.3 ± 0.3
0.47[f]	32	28	0.07 ± 0.01	0.01 ± 0.002	0.04 ± 0.01	310 ± 22	1.8 ± 0.4	8.1 ± 0.5	2.1 ± 0.3

[a] Amounts of Tsr and Tar are expressed as fractions of the total protein content of the membrane preparations.

[b] ν_{max} is the maximum rate of production of pmol CheY-P·s^{-1}, normalized to 1% receptor.

[c] ν_{min} is the rate of production of pmol CheY-P·s^{-1}, normalized to 1% receptor, in the presence of saturating attractant (100 mM).

[d] Membranes containing Tar or Tsr were mixed at a ~ 1:1 ratio before use in the in vitro receptor-coupled kinase assay.

[e] Sequentially coexpressed Tar//Tsr at a ~ 1:1 ratio (see Figure 3) were used in the assay. Tar was expressed first.

[f] Sequentially coexpressed Tsr//Tar at a ~ 1:1 ratio (see Figure 3) were used in the assay. Tsr was expressed first.

[g] The n/a entry means that this parameter could not be determined for the sample.

DISCUSSION

E. coli cells sense and adapt to concentrations of chemoeffectors that range over five orders of magnitude *(11)*, and they can migrate purposefully even in very shallow chemical gradients *(65)*. To understand this and other comparable signal transduction systems fully, the basis of their exquisite sensitivity and plasticity must be determined. One possibility is that different receptors interact synergistically. In vitro and in vivo studies have shown high *(71, 91)* or low *(87)* receptor cooperativity in response to ligands, depending on the conditions used. Our results show that Tar and Tsr, at least in their QEQE configurations, cooperate to stimulate CheA kinase activity and that mixed populations of these two receptors give dramatically altered responses to attractant ligands compared to pure Tar or Tsr populations. Such synergistic interactions may increase the sensitivity of the system and expand the range of chemoeffector concentrations over which the cells respond.

Receptor amount affects CheA kinase activity. Our results confirm that the fraction of receptors relative to total protein in the cell membrane affects their behavior. Receptors expressed at low levels are apt to be more randomly scattered and isolated than receptors expressed at higher levels. We see a linear increase in Tar-stimulated and Tsr-stimulated CheA activity up to receptor fractions of 50% of total inner-membrane protein (Figure 2.1), suggesting that formation of ternary complexes and/or larger patches of receptors is favored as the receptor fraction increases. However, *E. coli* chemoreceptors expressed at normal levels localize to the cell poles, although not in

tight clusters *(49, 91, 92)*. This tendency could bring receptors together even at physiological levels of synthesis to create high local population densities.

Assemblages of overexpressed receptors are relatively stable. Receptor-stimulated CheA activities measured when membranes from cells expressing either Tar or Tsr were mixed were virtually the same as those seen when Tar and Tsr were expressed sequentially in the same cells (Table 2.2 and Figure 2.3). In contrast, when Tar and Tsr were expressed at the same time, they exhibited strong interactions that were seen both as synergistic stimulation of CheA activity (Figure 2.4) and as an increase in the amount of aspartate or serine required to inhibit CheA activity (Figure 2.5 and Table 2.3). In the case of sequential expression, the receptors had several hours in vivo and the entire time (> 24 h) of membrane preparation and the four-hour incubation with CheA and CheW in vitro to interact and switch partners. However, no significant synergistic interactions were observed under these conditions.

Structural studies *(35)* and genetic (*13*) and chemical-crosslinking *(36, 39)* analyses have suggested that receptors interact, through their cytoplasmic domains, to form trimers of dimers. One explanation for the lack of synergy between sequentially overexpressed Tar and Tsr is that they remain in relatively homogeneous patches so that trimers composed of the two types of receptors are unlikely to interact. Another possibility is that synergy requires association of Tar and Tsr in trimers of dimers that must be established during the initial assembly of the receptors into the membrane.

Electron micrographs of negatively stained inner membranes highly enriched for the QEQE from of Tsr (R.S. McAndrew, unpublished results) reveal that, in the absence

of CheA and CheW, Tsr is detected only as trimers of dimers. In the presence of CheA and CheW, hexagonal close-packed lattices of receptors appear, and trimers can be caught in the act of joining, or leaving, the lattices. Also, in crude preparations containing both inner and outer membranes, the C-terminal 35 residues are removed from about 50% of the population of QEQE Tsr (R.-Z. Lai, unpublished results). We propose that endogenous proteases retained in these preparations remove these flexible tails, which remain unresolved in the crystal structure of the QQQQ form Tsr (*12*). Within trimers of dimers, only half of the tails may be accessible, with the tail of one subunit of a dimer pointing outward from the trimer axis and the tail of the other subunit pointing in toward the center of the trimer, where it is protected. The finding that the 50% truncation is highly reproducible and that incubation at room temperature for 24 h does not lead to a significant increase in truncation suggests that these trimers of dimers are quite stable.

We realize that this interpretation may seem at odds with conclusions drawn from in vivo chemical crosslinking experiments that suggested that Tar and Tsr can exchange among trimers in the absence of CheA and CheW *(39)*. The explanation may lie with different levels of receptor expression, which were high in the protease-protection and electron-microscopy analyses and were at physiological levels in the crosslinking experiments. Clearly, a concerted and carefully controlled study will be required to resolve the issue, but the failure of sequentially expressed Tar and Tsr to show functional interactions is at least consistent with the stability of trimers of receptor dimers in the absence of CheA and CheW.

Co-expressed Tar and Tsr stimulate CheA synergistically. Sourjik and Berg *(71)* recently reported that increased expression of Tar in the presence of Tsr increases CheA activity in vivo. Our in vitro data are consistent with their results and support the idea that a mixture of receptors enhances receptor-dependent stimulation of CheA. In particular, a Tar/Tsr dimer pair may support more CheA activity than a Tar/Tar or Tsr/Tsr dimer pair.

We imagine two possible reasons for the enhanced activity of a mixed dimer pair. First, a ternary complex formed by a Tar/Tsr dimer pair may have higher specific activity than a complex formed by a Tar/Tar or Tsr/Tsr dimer pair. Second, a Tar/Tsr pair might have a higher affinity for CheW and/or CheA than a Tar/Tar or Tsr/Tsr pair. We favor the latter interpretation because the change in CheA-stimulating activity of Tsr in different states of covalent modification is due to altered affinity of the different forms for CheA and CheW rather than to the specific activity of the ternary complexes once made *(54)*.

To model synergy between Tar and Tsr, we developed a computer program that generated an approximation of the CheA activity curve shown in Figure 2.4. The simulation is based on the existence of trimers that contain both Tar and Tsr dimers. We note that the electron micrographs described above suggest that the integrity of trimers of dimers can be lost in the presence of CheA and CheW and that the actual signaling unit may be an extended hexagonal lattice of receptor dimers. Nonetheless, since the receptors appear to be delivered to these lattices as trimers of dimers (R.S. McAndrew, unpublished results), the distribution of receptors within such arrays will be strongly

influenced by the composition of the trimers that serve as building blocks.

The simulation calculates the expected activity of mixed receptor populations based on two parameters. The first parameter is the relative probability of assembling ternary complexes at Tar/Tar, Tsr/Tsr and Tar/Tsr dimer interfaces. (The difference, if any, in the activity of a Tar/Tsr or Tsr/Tar interface should be irrelevant, since any mixed trimer contains one interface of each type. Thus, only the average activity of the two interfaces need be considered.) The second parameter is the probability of forming the four different trimers of dimers (Tar/Tar/Tar, Tar/Tar/Tsr, Tar/Tsr/Tsr, and Tsr/Tsr/Tsr). The program used to make these calculations is described in Material and Methods and, in more detail, in the Supplementary Material.

Figure 2.6 shows the best fit to our data generated by the program and also depicts the relative fraction of each of the four possible trimers of receptor dimers at all ratios of Tar to Tsr. The parameters that provided the best fit were:

Relative CheA activity (equivalent to CheA/CheW affinity) for Tar-Tar, Tsr-Tsr and Tar-Tsr mixed interfaces = 1: 2: 21. [We note that this is well within the range of values observed by Shrout and Weis *(54)* using receptors with different states of covalent modification.]

Relative affinity for trimer formation: Tar to Tsr = 1:100.

Using these parameters, the simulation yielded a peak activity when Tsr comprised 20% of the total receptor population. At this point, about 60% of the trimers are Tar/Tar/Tar, 25% are Tar/Tar/Tsr, 5% are Tar/Tsr/Tsr, and 10% are Tsr/Tsr/Tsr. Although dimers of dimers are presumably an intermediate in the formation of trimers of dimers, a

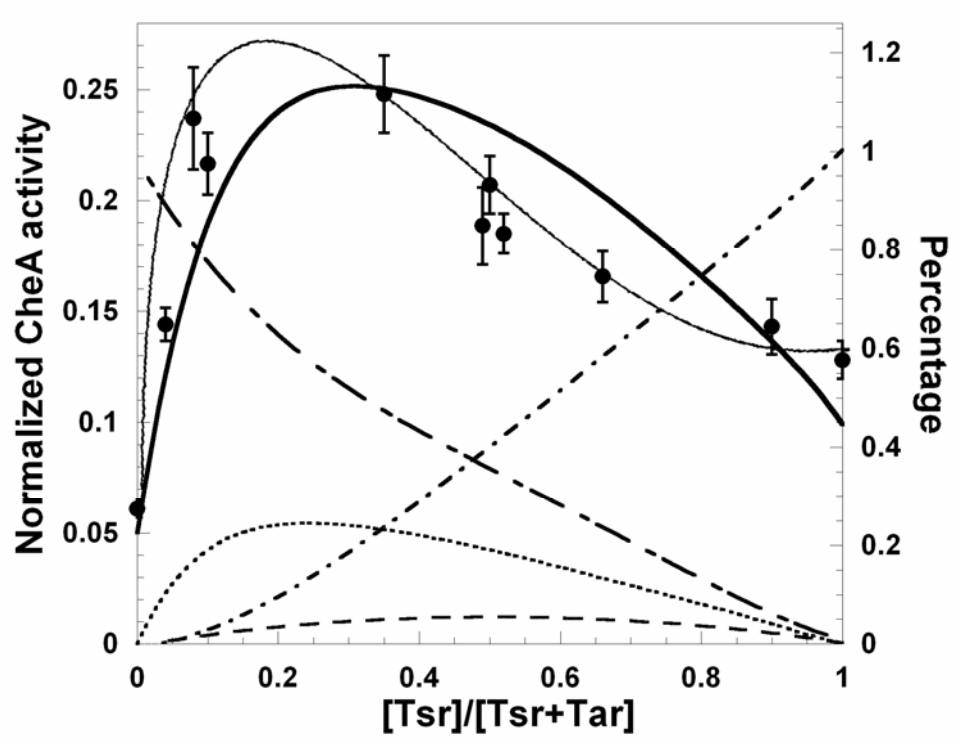

FIGURE 2.6 Computer-based simulation of CheA activity and receptor trimer formation. The assumptions used in the simulation are described in the text and in Supplementary Material. The thick solid line shows the CheA activity calculated from the simulation program. The thin solid line is the Beta-distribution fit for the experimental data from Figure 3. The fractions of trimer types at each ratio of Tar to Tsr are shown as follows: Tar/Tar/Tar, alternating short and long dashes; Tar/Tar/Tsr, dots; Tar/Tsr/Tsr, dashes; Tsr/Tsr/Tsr, alternating dots and short dashes.

simulation that took this step into account did not yield a curve significantly different from the one generated by the simpler program (J.M.B. Manson, data not shown).

A critical reader can protest that the simulation provides only a rough approximation to the experimental data. We suspect that the biggest factor is the oversimplification of considering only trimers of dimers. Within the larger receptor/CheA/CheW lattices found in our unpublished electron micrographs and predicted by the polar clustering of receptors observed in vivo (*6-8*) and theoretical considerations (*14, 20-23*), more complicated interactions of receptors can occur.

Distribution of trimers of dimers at different ratios of Tar to Tsr. Based on our experimental results and the simulation, we propose that the relationship of global CheA-stimulating activity, as calculated by the computer simulation, and the composition of the trimers of dimers at different ratios of Tar and Tsr will be approximately as shown in Figure 2.7. Tar-Tsr dimer interfaces support the highest activity because they have the highest affinity for CheA and CheW. Tar-Tar interfaces are the least active, and Tsr/Tsr interfaces support twice the activity of Tar/Tar interfaces. We suggest that Tsr forms trimers of dimers a hundredfold more readily than does Tar. This model is presented as a guide to further experiments, not as a definitive explanation, since it does not account quantitatively even for the data presented here.

The biological significance of chemoreceptor crosstalk. The ability of QEQE Tar and Tsr to interact synergistically to increase overall CheA activity confers no obvious advantage to *E. coli*, since each of these receptors, and presumably their $E^{m}EE^{m}E$ correlates, is capable of stimulating CheA on its own. However, Tar(EEEE) and

FIGURE 2.7 Model to explain receptor synergy. Tar and Tsr dimers are represented as closed and open circles, respectively. Their relative distributions are shown at the ratio that yields peak synergy (Tsr:Tar = 1:4) and at the ratio found in wild-type cells in vivo (Tsr:Tar = 2:1). The computer-generated curve of predicted CheA-stimulating activities at different Tar:Tsr ratios is the same as in Figure 5. We propose that the composition of a dimer interface determines the CheA activity associated with it, either because of differences in the specific activity of the receptor/CheA/CheW ternary complex or because of differences in the affinity for CheA and CheW. The ratio of 1:2:21 for the activities at Tar:Tar, Tsr:Tsr, and Tar:Tsr (Tsr:Tsr) interfaces gave the best fit to the data. The skew of the synergistic peak toward a Tar:Tsr ratio > 1:1 required the assumption that different receptor dimers incorporate into trimers with different affinities. The best fit was achieved with relative probabilities of formation of 1:1:1:100 for Tar/Tar/Tar, Tar/Tar/Tsr, Tar/Tsr/Tsr, and Tsr/Tsr/Tsr, respectively. However, the curve changed little when the relative probability of formation of Tsr/Tsr/Tsr trimers was varied over a range from 20 to 1,000 times the probabilities of formation of the other three trimers of dimers.

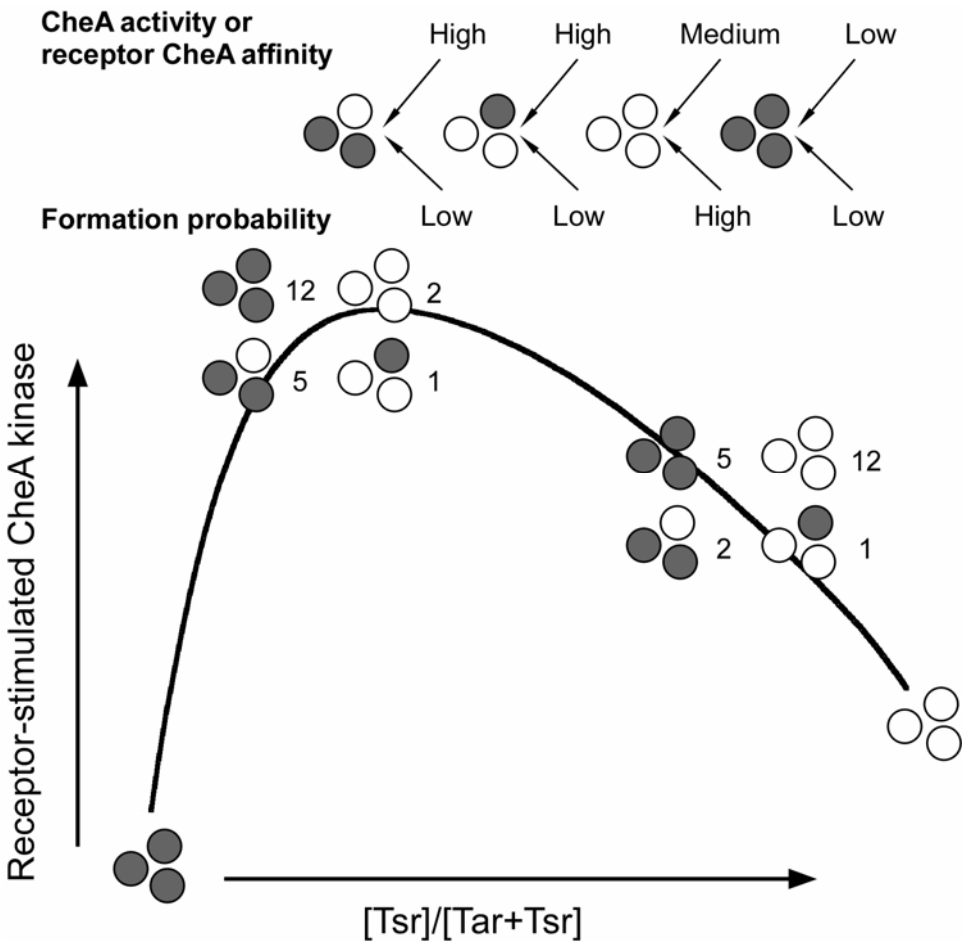
CheA activity or
receptor CheA affinity
High
High
Medium
Low
Low
Low
High
Low
Formation probability
12
2
5
1
5
12
2
1
Receptor-stimulated CheA kinase
[Tsr]/[Tar+Tsr]

Tsr(EEEE) have much lower intrinsic CheA-stimulating ability than their QEQE or QQQQ derivatives *(71)*. Tar(EEEE) and Tsr(EEEE) each is capable of synergistic enhancement of the in vitro CheA-stimulating activity of the QEQE form of their opposite number (R.-Z. Lai, unpublished results), and presumably also of the $E^{m}EE^{m}E$ forms in vivo. Moreover, the low-abundance receptors Tap and Trg cannot mediate chemotaxis as sole transducers in the cell (*50,51*). We intend to test whether they also are capable of synergistic stimulation of CheA activity by Tar(QEQE) and Tsr(QEQE). If so, this ability would permit them to function as actively contributing members of the receptor patch.

The fact that the greatest amount of synergy is seen at a ratio of Tsr:Tar of 1:4 rather than the normal in vivo Tsr:Tar ratio of 2:1 is not particularly troubling. Within an extended lattice, different neighborhoods will presumably show considerable variation in receptor composition. The mechanism of protein synthesis, in which multiple polypeptides are translated from a single mRNA, will contribute to a lack of uniformity, provided that dimers do not readily exchange among trimers. Even if dimers do exchange among trimers in a stochastic fashion, local variations will arise. Thus, within a signaling lattice or a collection of signaling lattices, there will likely be patches enriched for Tar, for Tsr, and possibly for Trg and Tap.

Through interactions among receptor types, attractant ligands sensed by lightly methylated or low-abundance receptors may be able to shut off a significant amount of CheA activity. When added to membranes containing mixtures of Tar(EEEE) and Tsr(QEQE) in ternary complexes with CheA and CheW, saturating concentrations of

aspartate inhibit a large fraction of receptor-coupled CheA activity (R.-Z. Lai, in preparation). Similarly, saturating concentrations of serine to membranes containing Tsr(EEEE) and Tar(QEQE) inhibits a large fraction of receptor-coupled CheA activity. We intend to test whether the same behavior is seen when low-abundance receptors, engineered to bind small-molecule ligands directly *(93-95)*, are mixed with the QEQE forms of Tar or Tsr and then exposed to attractants sensed by the low-abundance receptors.

A final, and perhaps the most important, advantage of synergy is suggested by the data presented in Figure 2.5. The IC_{50} for aspartate in mixed Tar/Tsr membranes can be up to 10^4 fold higher than it is with a pure population of Tar, and the IC_{50} for serine can be up to 10^2 fold higher than it is with a pure population of Tsr. We speculate that this lower sensitivity, and the decrease in the apparent Hill coefficient from 2 to 1 (Table 2.3), reflects different responses of receptors to their ligands depending on their local environment. At the 2:1 ratio of Tar to Tsr found in wild-type cells *(17)*, our simulation predicts that ~25% of the trimers should be Tar/Tar/Tar, ~10% Tar/Tar/Tsr, ~5% Tar/Tsr/Tsr, and ~60% Tsr/Tsr/Tsr (Figure 2.7). The broad range of attractant concentrations sensed by these different combinations of receptors may augment adaptive methylation to achieve optimal monitoring of the chemical gradients *E. coli* encounters during its normal enteric existence.

CHAPTER III

TALE OF A CHEMORECEPTOR TAIL

SYNOPSIS

The key control step in the chemotaxis of *Escherichia coli* is regulation of CheA kinase activity by a set of four transmembrane chemoreceptors. The receptor/CheA/CheW ternary complex can be viewed as an allosteric enzyme whose activity is regulated by the binding of attractant or repellent to the periplasmic domain of the receptor. Kinase activity is also modulated by reversible methylation of the receptor during the adaptation process. The C-terminus of the aspartate chemoreceptor (Tar), including the structurally dynamic C-terminal tail and the C-terminus of the cytoplasmic helix-2 (CD2) is potentially accessible to two regions known to be important for receptor function: the HAMP linker and the adaptation sub-domain. The C-terminus of Tar has generally been regarded as a linker for the NWETF pentapeptide, which is the binding site for the CheR and CheB methylation/demethylation enzymes. However, the receptor C-terminus is also a potential contributor to transmembrane signaling. Here, we present a mutational analysis of the C-terminus of Tar. The more residues that were deleted in this region, the less sensitive Tar became to inhibition by aspartate. Tar containing a deletion extending from residue 505 to the beginning of, or through, the NWETF sequence still stimulated CheA but failed to be inhibited by aspartate. Deletions starting with residue 513 increased the K_i for aspartate 10 fold. Neutralization of any one of four basic residues in this region (K523A, R529A, R540A, R542A) increased CheA

activation, whereas the R505A substitution decreased CheA stimulation by 40% and decreased the K_i for aspartate up to 8 fold. The R505E substitution completely abolished the ability to stimulate CheA. These results implicate the receptor C-terminus in maintenance of baseline receptor activity and in attractant-induced transmembrane signaling. They also suggest how adaptive methylation might counteract the effects of attractant binding.

INTRODUCTION

Bacterial chemotaxis is the best-developed model system for transmembrane signal transduction. Like many other signaling systems, bacterial chemotaxis regulates a protein kinase *(57-59, 71, 96)*. Regulation is carried out by a group of transmembrane chemoreceptors that sense stimuli, generally at the outer surface of the cell membrane, and transmit signals into the cytoplasm. The interaction of the CheA kinase with the receptors requires the coupling protein CheW. A ternary complex, consisting of receptor/CheW/CheA, is active in its apo form and is regulated by the binding of attractant (inhibitory ligand) or repellent (activating ligand) to the receptor *(61, 90)*. The receptor stimulates ATP-dependent autophosphorylation of CheA, which then transfers the phosphoryl group to the response regulator CheY. Binding of phospho-CheY to the FliM protein in the C-ring of the flagellar motor increases the probability of clockwise (CW) flagellar rotation and thereby the incidence of tumbling by the cell *(97)*. The activity of CheA in activating CheA is continually balanced by the activity of the phosphatase CheZ. The ratio of CW to counterclockwise (CCW) rotation depends

sensitively on the intracellular concentration of phospho-CheY *(22)* and sets the run-tumble swimming behavior of the cell *(16, 98)*.

Bacteria use methylation/demethylation, mediated by the CheR methyltransferase and the CheB methylesterase, to adapt to attractants and repellent, respectively *(99, 100)*. The adaptation system allows a cell to respond over a wide range of chemoeffector concentrations. Efficient covalent modification of a receptor requires the presence of a pentapeptide sequence, NWETF, which comprises the last five C-terminal residues of the aspartate (Tar) and serine (Tsr) receptors *(43, 56, 95)*. Even the isolated pentapeptide binds CheR and, with lower affinity, CheB *(40-43, 101)*. The steady-state methylation level of the receptors is determined by the relative activities of these two enzymes.

In *E. coli*, there are four membrane-spanning, homodimeric chemoreceptors: Tar, Tsr, Tap, and Trg. The intracellular level of the high-abundance receptors Tar and Tsr is about 10-fold higher than that of the low-abundance receptors, Tap and Trg *(17, 102, 103)*. All of these receptors contain a periplasmic domain, a transmembrane region, and a large cytoplasmic domain (Figure 3.1) *(104)*.

The major part of the cytoplasmic domain consists of two anti-parallel α-helices (CD1 and CD2), which form a hairpin. Proceeding from the membrane into the cytoplasm, the cytoplasmic domain features the HAMP linker, the methylation sub-domain, and the kinase-activation sub-domain, as illustrated in Figure 3.1 *(35, 105)*. The HAMP linker contains two predicted amphipathic α-helices and connects the second transmembrane helix (TM2) to the cytoplasmic sub-domains *(106-108)*. The methylation sub-domain contains the four to five glutamyl residues that serve as methylation sites,

FIGURE 3.1 Schematic view of the Tar chemoreceptor showing engineered C-terminal truncations and residue substitutions. The model of Tar is based on crystal structures of the periplasmic domain of *Salmonella enterica* (Milburn *et al.*, 1991; Scott *et al.*, 1993) and *E. coli* (Bowie *et al.*, 1995) Tar and the cytoplasmic domain of *E. coli* Tsr (Kim *et al.*, 1999). Structures for the TM, HAMP linker, and extreme C-terminal region are not available, so their configuration in the diagram is only guesswork. The receptor is shown as a homodimer. Starting at the N-terminus, each monomer consists of transmembrane helix 1 (TM1, white); a periplasmic domain that is a four-helix bundle (α1 to α4); transmembrane helix 2 (TM2, black); a HAMP linker that consists of amphipathic helix 1 (AS1 light gray) and 2 (AS2, dark gray); a helical hairpin comprising the highly conserved signaling region; and a disordered C-terminal tail (thick black line) with the NWETF CheR/B binding motif (gray box) at its end. The right side of the figure represents the last 63 residues of *E. coli* Tar. The red stars indicate the six basic residues (five Arg and one Lys). The NWETF pentapeptide is depicted as a gray box, and the most C-terminal methylation site is shown as an open circle. Endo-truncations (ET) extend from one of the basic residues to just before the NWETF. The corresponding complete truncations (CT) have the same N-terminal ends but delete through the NWETF. In addition, each of the Arg and Lys residues was converted to Ala (*e.g.*, R541A), and Arg-505 was also converted to Glu (R505E).

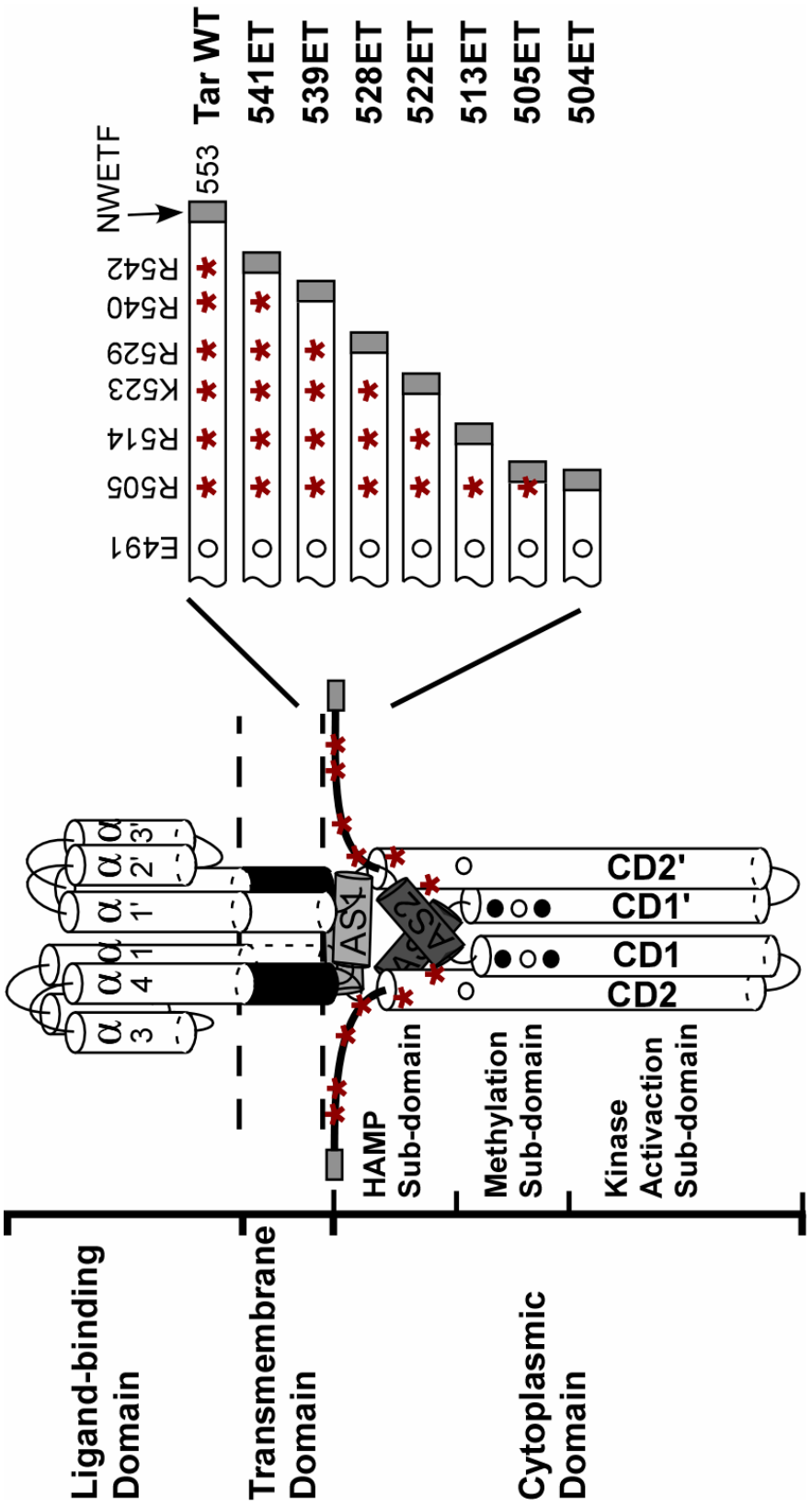
Tar WT
541ET
539ET
528ET
522ET
513ET
505ET
504ET
NWETF
553
R542
R540
R529
K523
R514
R505
E491
α 3
α α 4 1
α α 1' 2'
α α 2' 3'
AS1
AS2
CD2'
CD1'
CD1
CD2
HAMP Sub-domain
Methylation Sub-domain
Kinase Activaction Sub-domain
Ligand-binding Domain
Transmembrane Domain
Cytoplasmic Domain

and CheA and CheW bind to the kinase-activation sub-domain. The chemoreceptors form trimers of dimers *(36, 37, 105)* that localize to the cell pole and form tight clusters there in the presence of CheA and CheW *(49, 50)*. Trimers may contain dimers of different receptor types *(36-39)* and are apparently organized into large signaling lattices that obligatorily contain CheA and CheW *(53, 64, 71, 89)* and also at least some of the CheR, CheB, CheY, and CheZ proteins of the cell.

The receptor/CheW/CheA ternary complex can be viewed as an allosteric enzyme *(71, 109)*. It has been proposed that there are two states of the enzyme: "on" and "off." The equilibrium between these states is affected by several factors: ligand binding *(87, 110)*, methylation *(87, 91)*, association with CheA and CheW *(54, 111)*, and association with other receptors in a large signaling cluster *(36, 38, 89)*. Attractant binding causes a conformational change in the cytoplasmic domain of receptor that can be restored by methylation *(112, 113)*. However, it is still unclear how ligand binding and methylation work together to regulate CheA.

The role played in chemotaxis by the last ~50 C-terminal residues of the receptors, with the exception of the NWETF pentapeptide, is obscure. The receptor C-terminal tail is highly dynamic *(35)* and presumably remains close to the cell membrane and the HAMP linker. At one extreme, the residues between the last methylation site (residue 491 of Tar) and the NWETF could simply act as a flexible tether. At the other extreme, this region might be intimately involved in transmembrane signaling and adaptation. To address this question more closely, we carried out a mutagenic analysis of this portion of *E. coli* Tar. We created both internal and terminal deletions, starting with residue 505,

and also created a number of single substitutions of basic Arg and Lys residues in this region. The *in vivo* and *in vitro* properties of the mutant receptors were then examined.

Our results confirm that the receptor C-terminus plays an active role in transmembrane signaling. They also suggest a mechanism by which adaptive methylation may counter the inhibition of CheA stimulation that ensues upon attractant binding. Taken together, our findings provide insight into the contribution of an often-neglected component of the chemoreceptor to its function, at least in the case of the high-abundance receptors.

MATERIALS AND METHODS

Strains and plasmids. Strain RP3098 [Δ*(flhD-flhB)*4] *(73)*, a derivative of the *E. coli* K12 strain RP437 *(74)*, was used to prepare membranes containing high levels of chemoreceptors. It was also used to express the CheA protein for purification. Another derivative of RP437, strain VB13 [*thr*+ *eda*+ Δ*tsr7201 trg*::Tn10 Δ*tar-tap5201*], was used for assays of chemotaxis *(95)*. Strain BL21(λDE3) (Novagen) was used to produce CheY and CheW for purification. The λDE3 derivative of BL21 [F^- *ompT* $hsdS_B$ ($r_B^- m_B^-$) *gal dcm*] contains a prophage that encodes the T7 RNA polymerase gene under the control of the *lacUV5* promoter.

Plasmids pDM011 and pRD400 both are derivatives of pET24a(+) and contain the *cheY* or *cheW* gene, respectively, expressed from a T7 promoter. Plasmid pKJ9 carries an isopropyl-D-thiogalactopyranoside (IPTG) inducible *cheA* gene. Plasmid pCJTar was constructed by cloning wild-type *E. coli tar* into pCJ30, where it is expressed under

control of a *tac* (IPTG inducible) promoter. Plasmid pMK113 (Amp^r), a derivative of pBR322, carries *E. coli tar* under control of a modified *tar* (*meche* operon) promoter; it also has single-stranded origin of replication from phage M13 *(95)*. VB13 containing pMK113 (*Bam*HI) carries out good chemotaxis to aspartate and maltose *(95)*. Mutations were introduced into *tar* carried on pCJ30 and pMK113 using the site-directed mutagenesis protocol from Stratagene.

Chemotaxis swarm assay. The swarm assay was performed as described previously *(114)* using strain VB13 containing pMK113 or one of its mutant derivatives. The swarm diameter was measured at 30°C at 4 hr intervals from the time a ring first became visible for cells expressing wild-type Tar, and chemotaxis was scored as the rate of increase in swarm diameter in mm/hr. Swarms for each mutant were measured in triplicate.

In vivo receptor methylation level assay. Receptor methylation was analyzed according to Draheim *et al. (114)* using strain VB13 containing pMK113 or one of its mutant derivatives. Tar was detected on the nitrocellulose membrane with anti-Tsr *(95)* antiserum (primary) and goat-anti-rabbit conjugated with alkaline phosphatase (secondary). The methylation state was determined from the position of the bands visualized on the immunoblot. The migration rate of Tar during SDS-PAGE correlates to the extent of methylation, with the more highly methylated species migrating faster. An equal mix of the EEEE, QEQE, and QQQQ forms of Tar, contained in membrane preparations made in strain RP3098, was used as a standard.

Purification of chemotaxis proteins. CheA and CheY were purified as described

previously *(89)*. CheW purification was based on the methods of Hess *et al. (83)* and Stock et al. *(115)*. Cytoplasmic membranes containing over-expressed receptors were prepared based on a published method *(89)*, with the following modifications. The harvested cells were treated with 100μg/ml egg lysozyme on ice for 30 min before lysis in a French Pressure Cell operated at 18,000 psi. The lysate was centrifuged at 1200 × g for 15 min to remove debris. Membranes were pelleted by centrifugation at 30,000 × g for 1 hr, washed, and resuspended in 2 ml of a 25% (w/v) sucrose solution. The membranes were then fractionated, dialyzed, analyzed, and stored as described *(89)*.

In vitro CheA kinase assay. The receptor-coupled CheA assay was performed as described *(89)*, as was ligand-dependent inhibition of CheA activity. The experimental data for the aspartate titration of activity were fitted with the Hill equation, using Origin software, version 7.0. The apparent K_i and the Hill coefficient, n_H, were determined with the Levenberg-Marquardt method with the Origin software. Standard deviations of the mean for K_i and n_H values were calculated with $n \geq 3$.

RESULTS

Internal Deletions of the Tar C-terminus. The C-terminus of *E. coli* chemoreceptors is presumed to be far from the periplasmic ligand-binding site and the CheA activation site at the cytoplasmic tip of the receptor (Figure 3.1). This region is apparently not essential for CheA stimulation, since under suitable conditions the low-abundance chemoreceptors, Tap and Trg, which have shorter C-termini lacking the NWETF pentapeptide, stimulate kinase activity as well as the high-abundance

chemoreceptors, Tar and Tsr *(94)*. The one well-established function of the C-terminus is to tether the adaptation proteins, CheR and CheB, via the NWETF. However, there is evidence from an older study *(89)*, and also from a very recent one *(116)*, that the C-terminus of the high-abundance receptors functions in other receptor signaling properties as well.

To expand our understanding of the function of the C-terminus of Tar in chemotaxis, we generated a series of internal deletions in this region. Six of these residues are basic: five Arg and one Lys. We therefore focused our analysis on these residues, creating two sets of deletions (Figure 3.1) that remove successively larger numbers of the positively charged residues. In one set the NWETF at the extreme C terminus is retained (endo-truncations, designated ET), and in the other it is removed (complete truncations, designated CT).

Chemotaxis mediated by C-terminally truncated Tar. The swarm assay was used to assess the ability of a plasmid-encoded mutant Tar protein to restore chemotaxis to transducer-deleted (ΔT) strain VB13. The wild-type and mutant receptors were expressed from a modified form of the native *tar* (*meche* operon) promoter. Chemotaxis to aspartate, maltose, and glycerol (the last to observe aerotaxis mediated by the chromosomally encoded Aer receptor *(6, 117)* was assessed. Cells expressing any of the ET receptors formed smaller swarms in aspartate or maltose semi-soft agar (Figure 3.2). The more residues of Tar that were deleted, the less efficient the protein was in supporting chemotaxis, a result consistent with the results of Li and Hazelbauer *(116)*. These receptors were also less efficient in allowing Aer to mediate aerotaxis. Only the

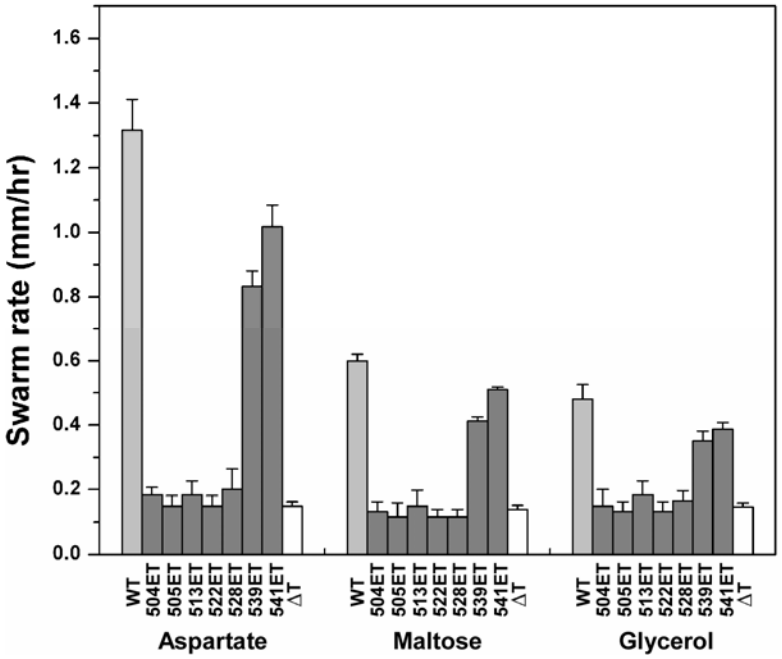

FIGURE 3.2 Chemotactic response mediated by wild-type and C-terminally endo-truncated Tar receptors. Rates of outward swarm-ring migration of VB13 (ΔT) cells expressing plasmid-borne wild-type or mutant *tar* genes were measured at 30^{o}C in mm/hr in minimal glycerol semi-solid agar containing 100 μM L-aspartate, 100 μM maltose, or with no additive (to measure aerotaxis). Assays were run in triplicate. Error bars represent the standard deviation of the mean.

539ET and 541ET receptors supported reasonably good chemotaxis, which was comparable on all three plates. The CT receptors, which lack the CheR/CheB binding site, all failed to support chemotaxis (data not shown).

Adaptive methylation of the ET receptors. Adaptive methylation was observed for each of the ET mutant Tar proteins in strain VB13. In the absence of chemoeffectors, wild-type Tar was primarily in the unmethylated state, with some of the singly methylated species also present (Figure 3.3). Addition of saturating (10 mM) $NiSO_4$ decreased the methylation level even further, whereas saturating (100 mM) aspartate increased methylation significantly. All the of the ET Tar proteins except the two most-truncated ones, 504ET and 505ET, were methylated to some extent in the absence of chemoeffectors, and all of these showed decreased methylation after addition of 10 mM $NiSO_4$. However, only the proteins with the smallest deletions, 539ET and 541ET, showed an increase in methylation level in response to the addition of 100 mM aspartate.

Stimulation of CheA kinase activity in vitro by ET receptors. We next examined the behavior of the truncated Tar proteins in the *in vitro* receptor-coupled CheA kinase assay. In the receptor-enriched (40-60% Tar) membranes used in this assay, CheR and CheB are absent and the receptors remain in their originally translated (QEQE) state of covalent modification at the methylation sites. In a previous study, the specific activity of receptors in stimulating CheA kinase increased linearly with the percent receptor relative to total membrane protein *(89)*. Therefore, in the current study we normalized the receptor activity to the ratio of Tar to total protein for each membrane preparation.

Most of the ET and CT receptors retained 80% or more of the CheA-stimulating

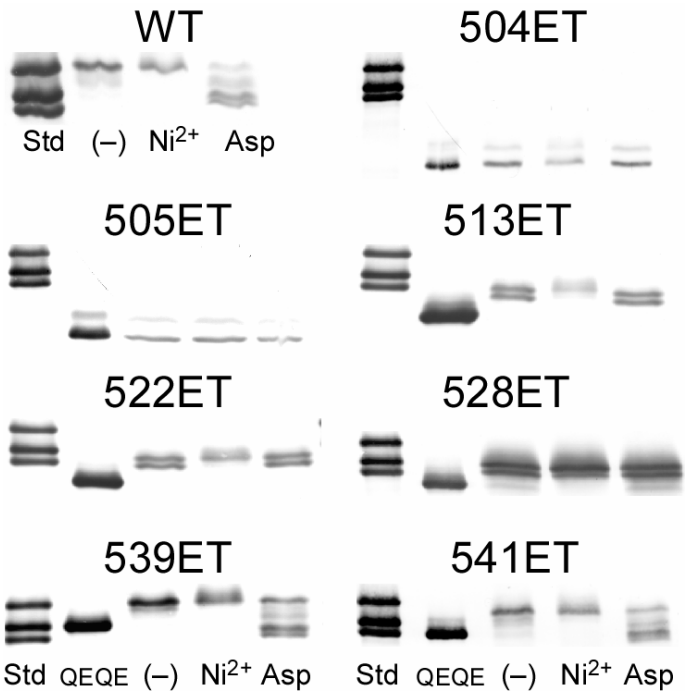

FIGURE 3.3 *In vivo* methylation of wild-type and C-terminally truncated Tar in response to chemoeffectors. Methylation of plasmid-encoded receptors was monitored in ΔT strain VB13 via immunoblotting. Membranes enriched for the EEEE, QEQE, and QQQQ forms of full-length Tar (migration-rate ladder) and the QEQE form of each truncated Tar were used as standards. Cells were exposed to 10 mM N_iSO_4 (repellent), 100 mM aspartate (attractant), or buffer (-). The gel was loaded with protein from equal numbers of cells for each strain.

activity of wild-type Tar (Figure 3.4). Even the 504ET and 504CT proteins had 70% of the wild-type activity. The only exception was the 513ET protein, which was less than 10% as active as the wild type. A similar result for a truncated Tar of the same length as 513CT, but with different residues at the last five C-terminal positions, was previously reported as having low activity in CheA stimulation *(116)*. None of the proteins appeared to be degraded significantly (Figure 3.3). These findings suggest that the low activity of 513ET is due to an inherent defect in its ability to stimulate CheA.

Truncated receptors are less sensitive to inhibition by aspartate in vitro. To test the susceptibility of the truncated receptors to inhibition by attractant, an aspartate titration of the *in vitro* Tar-dependent CheA activity was performed. Both the inhibition constant (K_i), which corresponds to the binding affinity for aspartate, and the cooperativity of the inhibition (n_H, the Hill coefficient) were measured. Wild-type Tar had a K_i of 7.5 ± 0.5 μM for aspartate. Both the ET and CT forms of 522, 528, 539, and 541 Tar had aspartate K_i values that were 1.5 to 3 fold higher (Table 3.1). The Tar 513 ET and CT receptors showed a substantially higher aspartate K_i of about 100 μM, but aspartate at higher concentrations still completely inhibited their ability to stimulate CheA (Figure 3.5). Remarkably, the 504ET, 504CT, 505ET, and 505CT proteins completely lost the ability to down-regulate CheA activity in response to aspartate. The cooperativity of aspartate inhibition also tended to decrease with increasing length of the truncations (Figure 3.5 and Table 3.1). Receptors lacking the NWETF pentapeptide (CT receptors) seemed to have a higher cooperativity for aspartate inhibition than their ET counterparts, but this pattern was not entirely consistent.

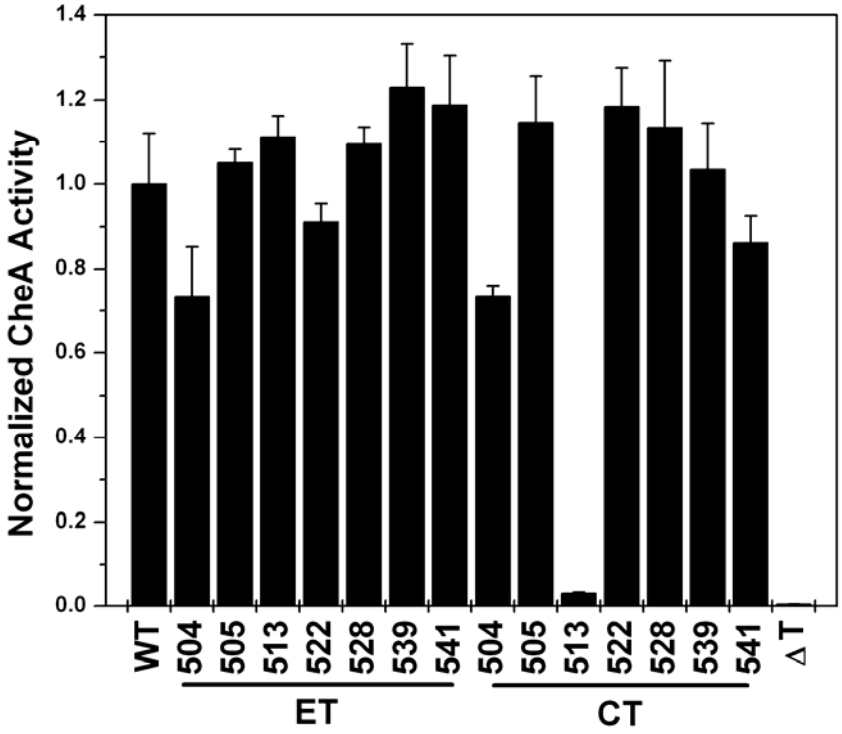

FIGURE 3.4 Relative CheA stimulation by C-terminally truncated Tar receptors. The ability of *in vitro* reconstituted receptor/CheW/CheA complexes to stimulate CheA kinase was assayed. Bars represent the activity stimulated by each receptor normalized to the activity supported by wild-type Tar. Assays were run in triplicate. Error bars represent the standard deviation of the mean.

Table 3.1 Effects of receptor C-terminal truncation on ligand response[a]

Receptor	K_i (μM)	n_H
Wild type	7.5 ± 0.5	2.0 ± 0.2
504ET	n/a[b]	n/a
505ET	n/a	n/a
513ET	101 ± 19	0.9 ± 0.1
522ET	9.4 ± 0.7	1.5 ± 0.1
528ET	15.9 ± 2.6	1.3 ± 0.1
539ET	24.1 ± 4.6	1.0 ± 0.1
541ET	14.9 ± 3.4	1.2 ± 0.1
504CT	n/a	n/a
505CT	n/a	n/a
513CT	100 ± 11	1.2 ± 0.1
522CT	10.1 ± 2.6	2.1 ± 0.4
528CT	12.3 ± 0.7	2.3 ± 0.3
539CT	13.9 ± 1.3	1.9 ± 0.1
541CT	16.6 ± 1.0	1.6 ± 0.1

[a] The half maximal inhibition concentrations K_i and the Hill coefficients n_H were estimated from the Hill equation.

[b] This parameter could be determined for this sample.

FIGURE 3.5 Effects of C-terminal truncations on aspartate inhibition of receptor-coupled CheA activity. The normalized CheA activities stimulated by (A) endo-truncation (ET) or (B) complete-truncation (CT) receptors were determined at a series of aspartate concentrations. A best-fit inhibition curve was calculated using the Hill equation. The receptors are indicated as follows: wild type (○), 504ET or CT (■), 505ET or CT (●), 513ET or CT (▲), 522ET or CT (▼), 528ET or CT (♦), 539ET or CT (⬢), 541ET or CT (⬟). Assays were run in triplicate. Error bars represent the standard deviation of the mean.

A

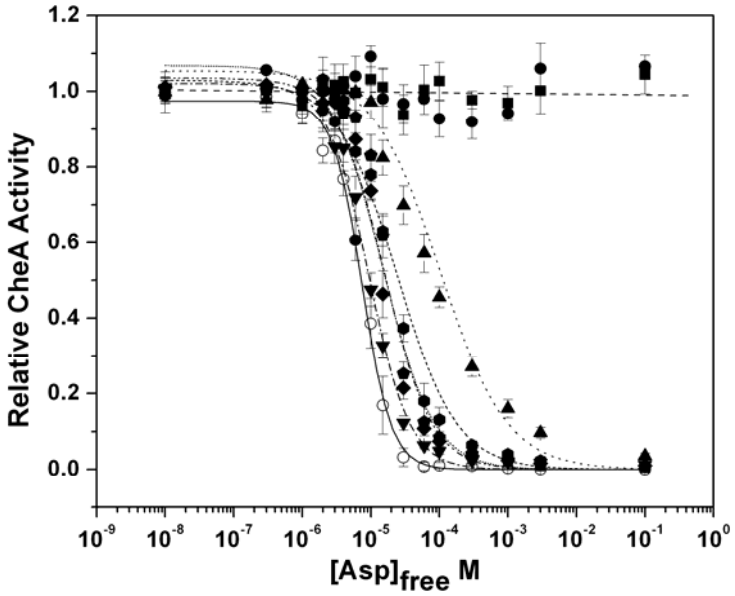
Relative CheA Activity
1.2
1.0
0.8
0.6
0.4
0.2
0.0
10^{-9} 10^{-8} 10^{-7} 10^{-6} 10^{-5} 10^{-4} 10^{-3} 10^{-2} 10^{-1} 10^{0}
$[Asp]_{free}$ M

B

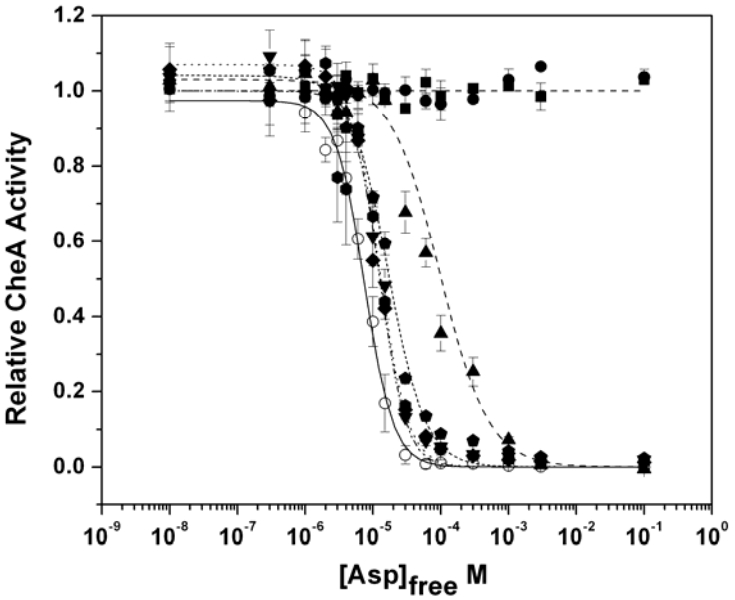
Relative CheA Activity
1.2
1.0
0.8
0.6
0.4
0.2
0.0
10^{-9} 10^{-8} 10^{-7} 10^{-6} 10^{-5} 10^{-4} 10^{-3} 10^{-2} 10^{-1} 10^{0}
$[Asp]_{free}$ M

Effect of Ala or Glu substitutions at basic residues. As noted earlier, the presence of six basic residues between residue 504 and the NWETF motif caught our attention, since they seemed to be candidates for interaction with either the Glu residues at the methylation sites or negatively charged anionic lipids in the cell membrane. Therefore, we replaced each of these six residues, singly, with Ala. Arg-505, which seemed likely to be crucial based on the behavior of the Tar504 proteins, was also replaced with Glu.

Plasmids expressing the Ala-substituted (or Glu-substituted) receptors from the modified *meche* promoter were introduced into strain VB13, and the transformants were subjected to the chemotaxis swarm assay. All of the receptors, with the exception of TarR505E, formed more-or-less wild-type swarm rings in aspartate, maltose, and glycerol semi-solid agar (Figure 3.6). VB13 cells expressing TarR505E formed aspartate swarms with only 50% of the diameter of those formed by cells expressing wild-type Tar or the other mutant Tar proteins. (The swarms of VB13/Tar505E on maltose and glycerol plates were similar to those of other strains.) Moreover, the aspartate swarms of cells expressing TarR505E had significantly sharper outer rings.

To determine in more detail how the Ala- and Glu-substituted receptors affect Tar, we examined their *in vivo* methylation levels, their baseline activities in the *in vitro* receptor-coupled CheA assay, and titration of their *in vitro* activity with aspartate. Most of the Ala-substituted proteins had methylation patterns just like that of wild-type Tar in the absence and presence of chemoeffectors (Figure 3.7). However, TarR505A and TarR505E had significantly increased levels of baseline methylation, a result that suggests that their signaling states may be shifted toward the “off”, or attractant-bound

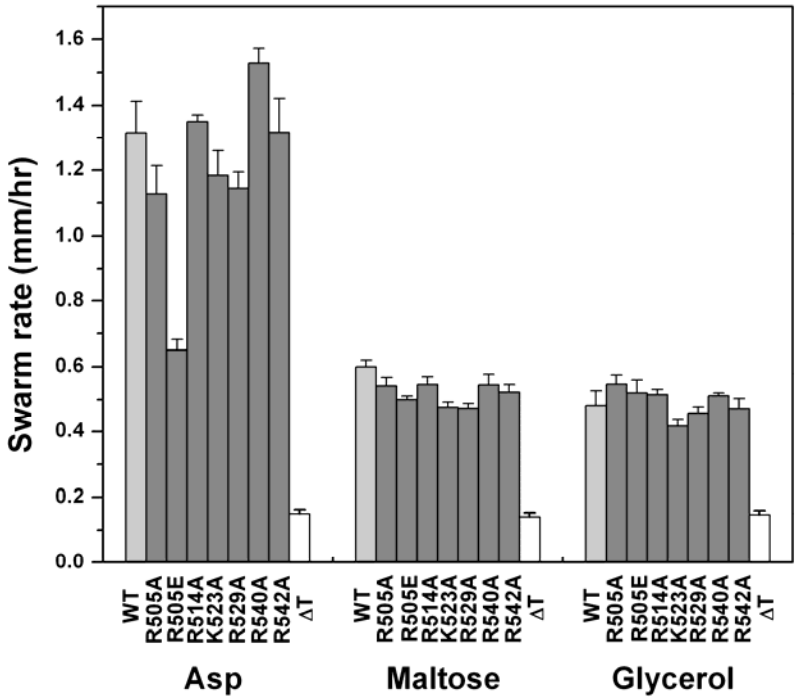

FIGURE 3.6 Effects on chemotactic behavior associated with residue substitutions at basic residues. Swarm assays were carried out as in Figure 2. The swarm rate at 30^{o}C was measured in mm/hr. Assays were run in triplicate. Error bars represent the standard deviation of the mean.

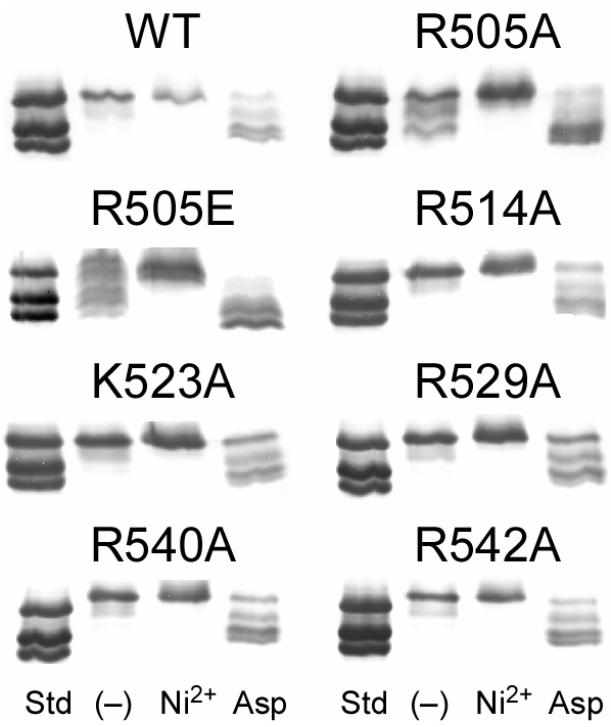

FIGURE 3.7 *In vivo* methylation of Tar receptors with single RA, KA, and RE substitutions Tar. The assay was performed as in Figure 3. Protein from equal numbers of cells of each strain was loaded in each lane.

state. However, both proteins could still respond to $NiSO_4$ and aspartate by decreasing or increasing their methylation levels, respectively.

In the receptor-coupled *in vitro* assay, all of the receptors had as high or higher a baseline activity as wild-type Tar (up to 60% higher for some), again excepting the proteins substituted at residue 505 (Figure 3.8). TarR505A had only 60% of the activity of wild-type Tar, whereas TarR505E had no significant CheA-stimulating activity at all. The ability of TarR505E to support some level of chemotaxis in the swarm assay indicates that the adaptive methylation seen *in vivo* can compensate to restore the ability of this receptor to activate CheA.

When the Ala-substituted receptors were titrated with aspartate *in vitro*, TarR505A exhibited a K_i of 1.1 ± 0.2 μM, which is seven-fold lower than the 7.5 μM K_i observed with wild-type Tar (Figure 3.9 and Table 3.2). In contrast, the other Ala-substituted receptors all showed somewhat higher (2 to 3-fold) aspartate K_i values than wild-type Tar. TarR505A had lower baseline activity and was more sensitive to aspartate inhibition than wild-type Tar, and the other Ala-substituted receptors have somewhat higher baseline activities and are slightly less sensitive to aspartate inhibition. Thus, the baseline CheA-stimulating and aspartate-inhibition properties of these mutant receptors are consistent with one another. A simple interpretation would be that Tar505A is slightly biased toward the “off” state, whereas the other Ala-substituted receptors are somewhat biased toward the “on” state. TarR505E is strongly biased toward the “off” state.

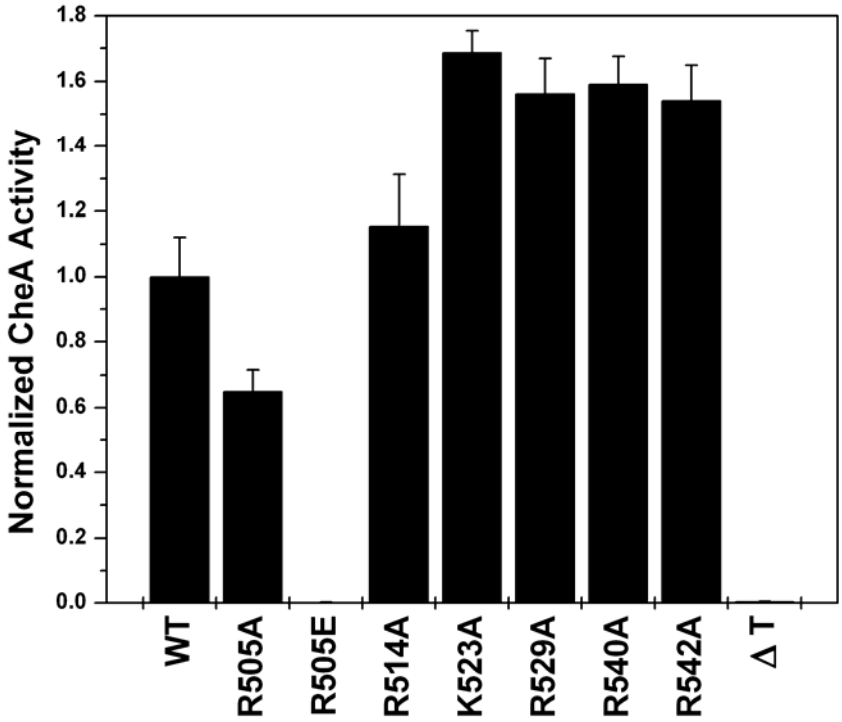

FIGURE 3.8 Relative CheA-stimulation activity by RA, KA, and RE-substituted Tar receptors *in vitro*. The activity of each mutant protein was normalized to the activity of wild-type Tar. Assays were run in triplicate. Error bars represent the standard deviation of the mean.

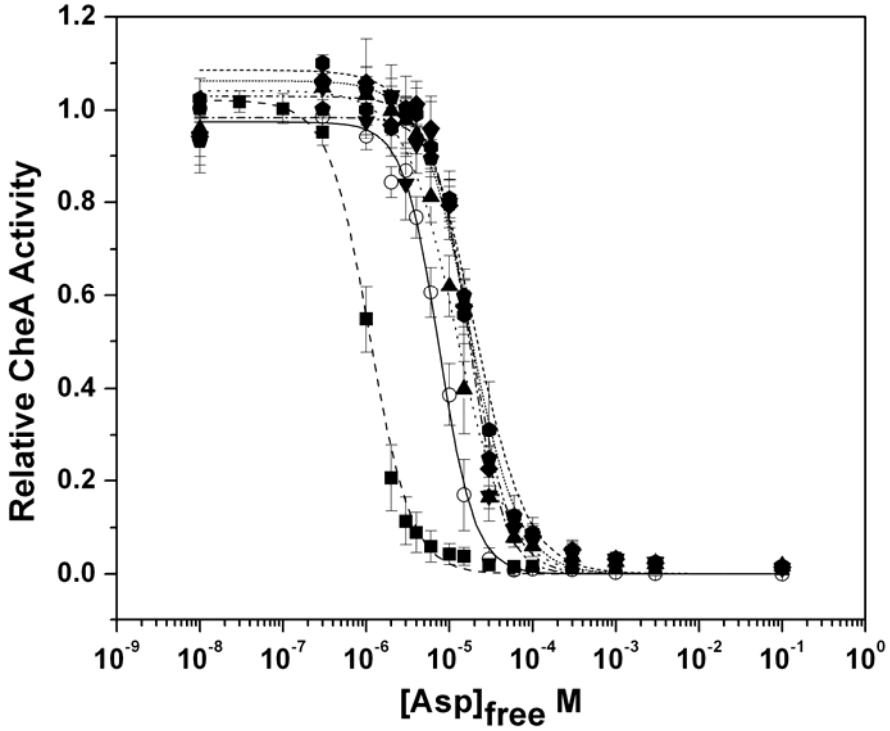

FIGURE 3.9 Effects of RA and KA substitutions on aspartate inhibition of receptor-coupled CheA activity. The *in vitro* titration inhibition assay was performed as in Figure 5. The different receptors are indicated as follows: wild type (○), R505A (■), R514A (▲), K523A (▼), R529A (♦), R540A (⬢), R542A (⬟). Assays were run in triplicate. Error bars represent the standard deviation of the mean.

Table 3.2 Effects of single residue substitution of basic residues at receptor C-terminus on ligand response[a]

Receptor	K_i (μM)	n_H
Wild type	7.5 ± 0.5	2.0 ± 0.2
R505A	1.1 ± 0.2	1.7 ± 0.2
R505E	n/a[b]	n/a
R514A	12.1 ± 3.7	1.4 ± 0.3
K523A	17.6 ± 2.0	2.1 ± 0.5
R529A	17.6 ± 2.2	1.8 ± 0.4
R540A	19.3 ± 3.3	1.4 ± 0.2
R542A	17.2 ± 3.2	1.5 ± 0.2

[a] The half maximal inhibition concentrations K_i and the Hill coefficients n_H were estimated from the ligand titrated CheA activity fitted with Hill equation.

[b] This parameter could not be determined for this sample.

DISCUSSION

The chemotaxis signaling pathway can be divided into four sequential events: stimulus detection by a receptor; transmission of the stimulus-induced conformational change in the receptor across the cell membrane; modulation of CheA kinase activity by the cytoplasmic domain of the stimulus-altered receptor; and adaptation by covalent methylation of the cytoplasmic domain of the receptor. Chemoattractants typically interact with the large periplasmic domain of a receptor at specific binding sites *(118-120)*. Small ligand-induced movements of the periplasmic domain are propagated across the membrane by the second transmembrane domain (TM2) of the receptor *(114, 121-125)* and are probably amplified into larger conformational changes within the HAMP linker domain *(107)*. The CheA and CheW proteins interact with the membrane-distal tip of the receptor dimer *(126)*, or trimer of dimers *(53, 127)*, in such a way that relatively subtle changes in receptor conformation increase or diminish CheA kinase activity. Finally, methylation of Glu residues at one or more of four independent sites, each consisting of a tandem pair of Glu residues *(113)*, leads to adaptation that cancels the ligand-induced signal by returning the CheA/CheW interaction sub-domain of the receptor to its pre-stimulus configuration.

The most C-terminal methylation site in the Tar chemoreceptor is Glu-491 *(35)*. The NWETF pentapeptide at the extreme C-terminal tail of Tar (residues 549-553) serves as a binding site for the enzymes that carry out adaptive methylation/demethylation: the CheR methyltransferase *(40, 43)*\ and the CheB methylesterase *(42)*. The function of residues 492 through 548, which link the

methylation sub-domain and the NWETF motif (see Figure 3.1) is much less well known. Residues 515 and beyond were not resolved in the crystal structure of the cytoplasmic domain of the closely related Tsr chemoreceptor *(35)*, so that a minimalist interpretation of the role of these residues is that they serve merely as a linker that joins the NWETF pentapeptide to the remainder of the receptor. However, several studies *(94, 95, 112, 116, 128, 129)* suggest that this portion of the receptor plays a more-active role in signaling.

Our detailed mutagenic dissection and manipulation of this region created a number of revealing alterations in the properties of Tar. The loss of chemotaxis by any receptor encoded by a *tar* gene deleted for the 15 bases corresponding to the NWETF pentapeptide was expected. It was also not surprising that substantially shortening the tether to the NWETF interferes with chemotaxis. Deletion of twenty or more residues preceding the NWETF (the 528ET to 504ET Tar proteins) almost eliminated chemotaxis to aspartate and maltose, and it also impaired the ability of Tar to assist Aer in carrying out aerotaxis (Figure 3.2). Even deletions removing only seven (541ET) or nine (539ET) residues impaired chemotactic swarming somewhat.

Correspondingly, the 528ET through 504ET receptors had abnormal patterns of methylation (Figure 3.3), especially following addition of aspartate. The 541ET and 539ET receptors, on the other hand, showed nearly wild-type patterns of methylation under all conditions (Figure 3.3). The lower level of methylation in response to aspartate could represent decreased accessibility of the NEWTF to CheR or a decreased ability of tethered CheR to reach the methylation sites. Deletions removing residues preceding the NWETF motif lower the affinity of the mutant receptor for CheR when the truncated

receptor resides in the membrane *(116)*. Since the isolated pentapeptide binds CheR with about the same affinity as the soluble cytoplasmic domain *(40)*, it is unlikely that the missing part of the receptor is directly involved in CheR binding. It seems more probable that access of CheR to the NWETF is somehow restricted in the ET receptors.

The receptor region corresponding to residues 515 to 548 of Tar is proposed to comprise random coils *(35)*. Because each receptor within the receptor patch is within the close range of other receptors, this C-terminal region is apt to interact with more stable structures to reduce its free energy. In fact, methylation has been shown to occur at least partly in *trans*, with CheR bound to one receptor using another receptor dimer as a substrate *(130, 131)*. The last 35, unstructured residues of the receptor C-terminal tail preceding the NWETF pentapeptide can potentially reach as far as 105 Å as an extended peptide chain, which is more than a sufficient length to allow interaction with the methylation sites, the cell membrane, and/or the HAMP linker. A shortened C-terminal tether might actually stabilize such interactions and reduce the accessibility of the NWETF pentapeptide to CheR. For the largest deletions, it could also create an opportunity for new interactions, such as between the NWETF pentapeptide and the N-terminal (membrane-proximal) part of the CD1 coiled-coil.

The true novelty of the data reported here is in what they tell us about the control of CheA activity, and propagation of the transmembrane signal by the C-terminus of Tar. Arg-505 clearly plays a pivotal role. Addition of Arg-505 to the 504ET receptor, to make the 505ET receptor, restored CheA kinase stimulation from 70% of wild-type levels to 100% of the wild-type level (Figure 3.4). Furthermore, the R505A replacement

lowered *in vitro* CheA stimulation by Tar to 60% of the wild-type level (Figure 3.8), and the R505E substitution entirely eliminated the ability of Tar to stimulate CheA *in vitro*. Titration with aspartate also showed that TarR505A was more sensitive to inhibition by aspartate, exhibiting a K_i of about 1 μM rather than 7 to 8 μM for the wild type (Figure 3.9 and Table 3.1).

The altered behavior of proteins with substitutions at position 505 was also observed *in vivo*. Cells expressing TarR505E as their sole receptor were severely impaired for aspartate taxis on swarm plates, and both TarR505A and Tar505E were more highly methylated *in vivo* (Figure 3.7), a result consistent with their baseline signaling state being biased toward "off." The crystal structure of the cytoplasmic domain of Tsr shows an Arg residue corresponding to Arg-505 of Tar located at the interface of CD1-CD2. We therefore propose that this basic residue stabilizes the interaction between CD1-CD2. We predict that this effect helps maintain the entire cytoplasmic domain in a tight coiled-coil that should push the equilibrium between the "on" and "off" signaling states toward "on," much as the electrostatic dynamic model *(132, 133)* proposes what neutralization of the Glu residues by methylation does during adaptation to an attractant signal. Substituting the basic residues at other positions with Ala has the modest but significant effect of biasing receptor toward "on" state. A similar effect was reported when certain negatively charged residues in methylation sub-domain were neutralized *(133)*. Both of these findings are consistent with the idea that the C-terminus and methylation sub-domain interact electrostatically.

The other side of the coin is the "lock-on" signaling properties of the 504ET and

CT (NWETF-deleted) and 505ET and CT receptors in the *in vitro* CheA-stimulation assay. The 513ET and 513CT receptors also show a Ki for aspartate of around 100 μM (Table 3.1), which is 12-fold higher than the 7.5 μM value of the aspartate K_i for wild-type Tar. The most-straightforward interpretation of this finding is that the loss of most of the C-terminal region interrupts coupling between the aspartate-induced transmembrane signal through TM2 and the kinase-activation sub-domain. One alternative is that the CD1/CD2 coiled coil, which makes up the bulk of the cytoplasmic portion of Tar, becomes more stable in the absence of the C-terminal region. One problem with this interpretation is that the proposed stabilizing effect of Arg-505 is absent in the 504 receptors. Another alternative is that removal of a large fraction of the NWETF tether could prevent an interaction of the C-terminal region with the membrane or the HAMP linker that is critical for propagating an attractant ("off") signal.

Figure 3.10 illustrates a possible mechanism by which the C-terminus of Tar involved in transmembrane signaling and methyl-dependent adaptation to attractant stimuli could counteract the inhibitory effect of ligand binding. This speculative model is based on the premise that the C-terminus interacts alternatively with the cell membrane and/or HAMP linker and with the methylation sub-domain to stabilize the "on" and "off" states of the receptor, respectively. We note that, although the NWETF pentapeptide is not required for receptor activity or transmembrane signaling, that it could form a short amphipathic helix that could lie parallel to cell membrane at the cytoplasmic polar/hydrophobic interfacial zone. This type of arrangement is common in anti-microbial peptides *(134)* and has been proposed for the "plug" of the MotAB proton

FIGURE 3.10 Model for the function of the C-termini of high-abundance chemoreceptors in control of CheA activity. Receptors are depicted as in Figure 1. The methylation/demethylation sites are represented as small circles; filled circles represent methylated glutamyl residues. We propose that, in the absence of ligand (A), AS1 of the HAMP linker associates with the membrane and the AS2 helices are in a tightly packed coiled coil (Butler *et al.*, 1998; Williams *et al.*, 1999) that helps stabilize the packing of the CD1 and CD2 helices. This conformation corresponds to the "on" state of the receptor. The potentially unstructured C-terminus of each subunit interacts with negatively charged anionic lipids at the membrane surface (shown) and/or the HAMP linker (not shown) to help stabilize the "on" state. When an attractant ligand binds (B), displacement of TM2 disrupts the association of the HAMP linker with the membrane, weakening the interaction of the C-terminus with the membrane and/or the HAMP sub-domain. This effect destabilizes the AS2 coiled coil and the tight packing of CD1 and CD2 from the two subunits. As a result the whole cytoplasmic domain becomes more dynamic, and the receptor moves into the "off" state. The positively charged portion of the C-terminal tail may interact with the methylation sub-domain in this state, as shown. Binding of CheR (large shaded oval) to the NWETF pentapeptide leads to methylation of the glutamyl residues, thus reducing the net negative charge in this region. This neutralization of negative charge decreases the electrostatic attraction of the C-terminal tail for the methylation sub-domain, allowing the receptor to return (D) to the "on" state.

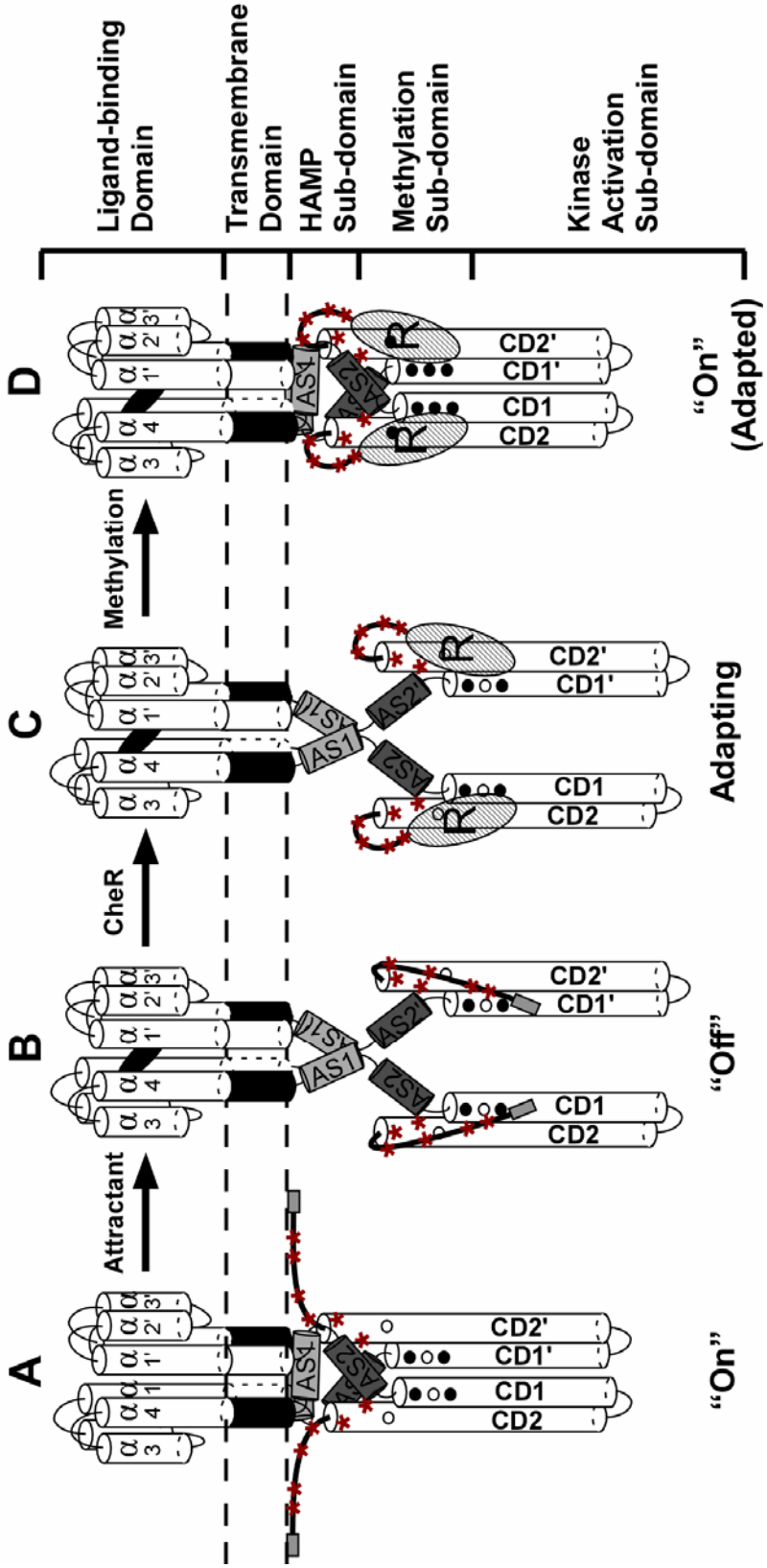
Ligand-binding Domain
Transmembrane Domain
HAMP Sub-domain
Methylation Sub-domain
Kinase Activation Sub-domain
A
B
C
D
Attractant
CheR
Methylation
"On"
"Off"
Adapting
"On" (Adapted)
CD2'
CD1'
CD1
CD2
AS1
AS2
R

channel of the *E. coli* flagellar motor *(135)*. This association could effectively sequester it from CheR when the receptor is in a CheA-stimulating state. The role of methylation would be to attenuate electrostatic interaction between the C-terminus and the methylation sub-domain to shift the signaling state back to "on" state.

Many of the details of this model remain to be tested and/or demonstrated, and it is presented not as an explanation but as a guide to future experimentation. It is noteworthy that basic amino acids are found within the last ~50 C-terminal residues of all thirteen Class I bacterial receptors that have been analyzed *(128)*. Thus, it seems highly likely that any ultimate explanation of receptor function will have to account for the contribution of the C-terminal region.

CHAPTER IV

CONCLUSIONS AND FUTURE DIRECTIONS

CONCLUSIONS

Over the course of billions of years, bacterial chemotaxis has evolved into a sophisticated protein-interaction system that converts stimulus input into directed motility. Transmembrane chemoreceptors interact with CheW and CheA to form the basic signaling unit. The signaling state is determined by the interaction of the receptors with CheA *(54)*. Such interactions are affected by other protein interactions: receptor with the membrane, C-terminus with methylation region or HAMP, receptor monomer with receptor monomer, and receptor homodimers with each other, etc. Thousands of receptors and CheA and CheW molecules cluster at the cell pole to form a higher-order signaling lattice. For the system to be sensitive enough to respond to changes in attractant concentration of 10 nM or less *(44, 45)*, it is crucial that each protein in the signaling lattice interact with many other proteins. To understand the control mechanism of the bacterial chemotactic system in detail, it is critical to understand interactions between individual proteins and within the system as a whole. The study of receptor function in bacterial chemotaxis is quickly developing on two scales: that of the individual receptor and that of the entire signaling system. I have dedicated the seven years of my Ph.D. study at Texas A&M to understanding these protein interactions at both levels.

Cross-talk among bacterial chemoreceptors. In Chapter II, I describe the

interaction between the Tar and Tsr chemoreceptors using an *in vitro* biochemical method. Both proteins are high-abundance receptors in *E. coli* and, as such, each can mediate chemotactic swarming in the absence of other receptors. Homodimers of Tar and Tsr can mix to form heterotrimers of dimers *(35, 132)*. The synergy between these two receptors in stimulating CheA confirms that chemoreceptors made simultaneously can engage in cross-talk. In the cell, all the chemotaxis and receptor genes are expressed at the same time, after the hook-basal body complexes of the motor are complete. Thus, all receptors should have an equal opportunity to form mixed trimers of dimers, which can then be incorporated into polar receptor patch. It has been shown that, once receptors incorporate into receptor patch in the presence of CheA and CheW, there is no further exchange of receptor dimers in the presence or absence of attractants *(37)*.

The peak synergy I observed occurred when Tar and Tsr dimers were present in unequal numbers, indicating that there is an unequal contribution by the two receptors. By itself, Tsr is twice as active as Tar in stimulating CheA *(89)*. However, the mix of receptors shows the highest CheA-stimulating activity at a Tar to Tsr ratio of 4 to 1. As discussed in Chapter II, one possible explanation is that Tar and Tsr contribute unequally to the formation of receptor trimers of dimers. However, it is still unclear whether the synergistic effect of CheA stimulation comes from interaction between receptor dimers within trimers or among trimers of dimers.

An informative expansion of this study would be to examine how the low-abundance receptors, Tap and Trg, interact with the high-abundance receptors, Tar and Tsr. Low-abundance receptors are present at 10 to 20 fold lower amounts than high-

abundance receptors. If our hypothesis about the preference for forming trimers of dimers holds true, the dominance of Tsr and Tar would make it almost impossible for Tap or Trg to form homotrimers of dimers.

The four MCPs in *E. coli* can, in principle, form up to 24 different trimers of dimers. If Aer is included, the number increases to 45. If, for examples, all Tar/Tsr and Tsr/Tar interfaces are considered equivalent, the four MCPs can form 20 types of trimers of dimers and 35 different trimers if Aer is present (Calculations were carried out with a computer simulation written by Josiah M. B. Manson, personal communication). Based on the relative abundance of the receptors *in vivo*, about 60% of the trimers of dimers will be Tsr homotrimers, ~25% be Tar homotrimers, and the majority of the rest will be Tsr-Tsr-Tar/Tap/Trg or Tar-Tar-Tsr/Tap/Trg, based on our simulation program *(89)*. Thus, almost all low-abundance receptors will be in trimers with high-abundance receptors. Although Trg, at least, can stimulate CheA kinase activity to a level similar to Tar *(56)*, neither Tap nor Trg supports chemotaxis independently. A maximal mixing of Tap, Trg, and Aer with high-abundance receptors could explain the "dependent" status of the low-abundance receptors. All of the low-abundance receptor dimers would have access to high-abundance receptors within a trimer, could be methylated through CheR/B bound to adjacent Tar/Tsr, and could propagate the signal initiated by ligand binding through the high-abundance receptors. This scheme could efficiently sense a broad spectrum of ligands with fewer total receptors than a mechanism without functional interaction.

The presence of Tsr dramatically affects the ligand response of Tar, and vice versa,

decreasing ligand sensitivity up to 10^4-fold. This result suggests that an important function of the signaling cluster is to expand the dynamic range of receptors. Of the 35 or 45 possible types of trimers, the majority will be homotrimers of high-abundance receptors. The receptors within these homotrimers have high affinity to ligand, whereas receptors in heterotrimers would have much lower affinity. Therefore, the cell is able to sense a low concentration of ligand with homotrimers and can respond to higher concentrations via sensing by heterotrimers. If local regions have different compositions of trimer types, the range of attractant concentrations that can be detected would be expanded even further.

The ability of low-abundance receptors to take advantage of high-abundance receptors imposes a potential problem in sensing ligand. If they behave like Tar and Tsr, they should have a low ligand affinity due to the heterotrimer formation. However, both Tap and Trg sense their ligands via periplasmic ligand binding proteins. The high ligand affinity of the ligand binding protein, coupled with a lowered affinity of the chemoreceptor for the binding protein, could easily compensate for this problem. In fact, *in vivo* measurements of the interaction between Tar and maltose-binding protein have shown that the binding is weak (apparent K_d of around 200μM MBP) *(136)*.

This study used receptors only in the QEQE modification state. In a cell, receptors are constantly being modified by the CheR and CheB enzymes, so they are present in different modification states. Different modification states imply different signaling states and different ligand-dissociation constants *(91, 114)*. Coupling the different covalent modification states with the CheA stimulation and mixed-receptor effects on

ligand sensitivitiy could be the key to explaining the sensitivity of the chemotactic system predicted by several mathematic models *(70, 71, 137, 138)*.

The receptor C-terminus is involved in modulating receptor signaling. As an allosteric enzyme, the tertiary complex of receptor, CheA, and CheW is affected by many factors besides interactions among receptors. In Chapter III, I describe a study that characterized the role of the last 50 residues at the Tar C-terminus. The C-terminus of Tar is close to the cell membrane and the HAMP linker, and it has the potential to be an important factor in signal modulation.

Removing the last 50 residues of the Tar C-terminus eliminates the ability of the receptor to signal in response to attractant binding, although the ability to stimulate CheA kinase remains normal. The stability of the truncated receptors and their retention of CheA-stimulation activity suggest that the receptor is unable to assume the "off" signaling state without its C-terminus. Perhaps the C-terminus stabilizes the "off" state. Shortening the receptor C-terminus also results in decreased receptor methylation in the presence or absence of chemoeffectors. This phenotype has also been addressed by the Hazelbauer group *(116, 129)*.

The involvement of the C-terminus in the adaptation process suggests that the C-terminus may interact with the methylation region, which is highly negatively charged. Another candidate for interaction with the C-terminus is the cell membrane, where polar head groups are also negatively charged. We hypothesize that the C-terminus interacts with these other moieties via electrostatic interaction. Replacing each of the six basic residues in the C-terminus with alanine had little effect on CheA-stimulation or ligand

response to attractant, except for the R505A substitution. This receptor is shifted slightly toward the "off" signaling state and is more sensitive to inhibition by aspartate. Substituting Arg-505 with Glu shifts the receptor strongly toward the "off" state, leading to a higher methylation level in the absence of ligand and eliminating CheA-stimulation activity *in vitro*. Residue Arg 505 points toward a potential interface between the HAMP and CD2. Therefore, Arg 505 might interact with the HAMP sub-domain to stabilize the "on" state of the receptor.

Similar effects on receptor signaling were observed when charged residues in the HAMP sub-domain were substituted or introduced, e.g., the E248K and G235D replacements in Tsr *(139)*. Although, it is not clear what interaction was interrupted by those mutations, this result suggests a potential experimental direction. Overall, the evidence suggests that the receptor C-terminus is an important modulator of chemotactic signaling.

FUTURE DIRECTIONS

Effects of covalent modification on functional interaction among receptors. Adaptation is an integral part of chemotactic signaling. Receptors in the EEEE form have very low CheA-stimulation activity and high affinity for attractant ligand. The QQQQ Tsr receptor, which mimics fully methylated Tsr, has high CheA-stimulation activity and low affinity for serine *(91)*. Receptors *in vivo* are present in different modification states, even in the absence of chemoeffectors. In order to understand the interactions among chemoreceptors, it is crucial to examine receptors in different

modification states. Of particular interest in this regard will be the behavior of Tar(EEEE)/Tsr(EEEE) and Tar(QQQQ)/Tsr(QQQQ) mixtures, as well as combinations of the (QQQQ) forms of either receptor with differently modified forms of the other. It will also be informative to examine the interaction between Tar(EEEE)/Tsr(QEQE), and Tar(QEQE)/Tsr(EEEE). I would predict that even the EEEE receptors can synergistically interact with QEQE receptors to stimulate CheA kinase.

Determine the active complex formed by co-expressed receptors in vitro. To understand interactions among chemoreceptors, it will be important to distinguish the contribution of each receptor within the cluster. The study that I described in Chapter II examined the behavior of the receptors *in vitro* at a fixed ratio of receptor to CheA and CheW. As an extension of that study, a pull-down assay could be used to assess the amount of CheA and CheW that actually binds to the receptors at different ratios of Tar to Tsr. That experiment could answer the question of whether the synergistic activation of CheA observed is due to the higher CheA specific activity or formation of more signaling complexes. This experiment should be performed together with direct ligand-binding measurements. As discussed in previous chapters, the amplification of the chemotactic signal is measured by the change in output relative to ligand occupancy of the receptors. Not all the receptors in our *in vitro* assay can form active signaling complexes with CheA and CheW because the ratio of receptor:CheA:CheW in our assay is 4:1:4. Therefore, not all ligand binding can be measured by inhibition of CheA. Combining measurements of kinase activity, ligand binding, and ligand-induced inhibition of kinase activity should produce information about the contribution of each

receptor type to kinase stimulation and ligand response.

Study the interaction between high-abundance and low-abundance receptors. The requirement that a high-abundance receptor be present for low-abundance receptors to mediate chemotactic swarming makes it especially interesting to study cross-talk between low- and high-abundance receptors. One potential problem is that the natural low-abundance receptors, Tap and Trg, require periplasmic binding proteins to respond to ligand. This problem can be circumvented by using the Tar-Tap hybrid receptor Tarp *(95)* and the Tsr-Trg hybrid receptor Tsrg *(94)*. These hybrid receptors have the cytoplasmic domain of the low-abundance receptor and the periplasmic domain of the high-abundance receptors. Thus they bind ligand directly in their perplasmic domains but should have the cytoplasmic interaction of the low-abundance receptors.

Test the interaction between the receptor C-terminus and the HAMP sub-domain. One important unresolved question is whether the receptor C-terminus modulates the signaling state of the receptor. A tempting hypothesis is that the C-terminus interacts with the HAMP sub-domain that links TM2 to the cytoplasmic signaling domain. Such an interaction could stabilize or destabilize HAMP. I identified two residue substitutions (Tar R505A and R505E) that shift the receptor toward the "off" state. Suppressing mutations in the HAMP sub-domain might restore normal signaling to strains expression R505A/E Tar. We could also use cysteine disulfide crosslinking to probe the C-terminus/HAMP interaction by introducing Cys residues at different locations in both the receptor C-terminus and the HAMP sub-domain.

Test whether the C-terminus interacts with the cell membrane to modulate

signaling. Cys residues introduced in the C-terminal tail of the receptor can be used to label the receptor with thiol-reactive fluorescent probes *(140)*, e.g. *N*,*N*`-dimethyl-*N*(acetyl)-*N*`-(7-nitrobenz-2-oxa-1,3-diazol-4-yl) ethylene diamine (NBD) *(141)*. NBD emits light at different wavelengths in aqueous and hydrophobic environments. This experiment can be done in the presence and absence of CheA and CheW, and with or without ligand. This study should be able to determine whether the receptor C-terminus interacts with cell membrane, and, if it does, whether the interaction changes under different signaling conditions.

REFERENCES

1 Berg, H. C., and Anderson, R. A. (1973) Bacteria swim by rotating their flagellar filaments, *Nature 245*, 380-2.

2 Meister, M., Lowe, G., and Berg, H. C. (1987) The proton flux through the bacterial flagellar motor, *Cell 49*, 643-50.

3 Berg, H. C., and Brown, D. A. (1972) Chemotaxis in *Escherichia coli* analysed by three-dimensional tracking, *Nature 239*, 500-4.

4 Tso, W. W., and Adler, J. (1974) Negative chemotaxis in *Escherichia coli*, *J Bacteriol 118*, 560-76.

5 Maeda, K., Imae, Y., Shioi, J. I., and Oosawa, F. (1976) Effect of temperature on motility and chemotaxis of *Escherichia coli*, *J Bacteriol 127*, 1039-46.

6 Bibikov, S. I., Biran, R., Rudd, K. E., and Parkinson, J. S. (1997) A signal transducer for aerotaxis in *Escherichia coli*, *J Bacteriol 179*, 4075-9.

7 Adler, J., Hazelbauer, G. L., and Dahl, M. M. (1973) Chemotaxis toward sugars in *Escherichia coli*, *J Bacteriol 115*, 824-47.

8 Manson, M. D., Blank, V., Brade, G., and Higgins, C. F. (1986) Peptide chemotaxis in *E. coli* involves the Tap signal transducer and the dipeptide permease, *Nature 321*, 253-6.

9 Adler, J. (1966) Chemotaxis in bacteria, *Science 153*, 708-16.

10 Adler, J. (1966) Effect of amino acids and oxygen on chemotaxis in *Escherichia coli*, *J Bacteriol 92*, 121-9.

11 Adler, J. (1969) Chemoreceptors in bacteria, *Science 166*, 1588-97.

12 Mazzag, B. C., Zhulin, I. B., and Mogilner, A. (2003) Model of bacterial band formation in aerotaxis, *Biophys J 85*, 3558-74.

13 Hirota, N., and Imae, Y. (1983) Na+-driven flagellar motors of an alkalophilic *Bacillus* strain YN-1, *J Biol Chem 258*, 10577-81.

14 Berg, H. C. (1996) Symmetries in bacterial motility, *Proc Natl Acad Sci USA 93*, 14225-8.

15 Wisdom, J. (2003) Swimming in spacetime: motion by cyclic changes in body shape, *Science 299*, 1865-9.

16 Sourjik, V., and Berg, H. C. (2002) Binding of the *Escherichia coli* response regulator CheY to its target measured in vivo by fluorescence resonance energy transfer, *Proc Natl Acad Sci USA 99*, 12669-74.

17 Koman, A., Harayama, S., and Hazelbauer, G. L. (1979) Relation of chemotactic response to the amount of receptor: evidence for different efficiencies of signal transduction, *J Bacteriol 138*, 739-47.

18 Clarke, S., and Koshland, D. E., Jr. (1979) Membrane receptors for aspartate and serine in bacterial chemotaxis, *J Biol Chem 254*, 9695-702.

19 Barak, R., and Eisenbach, M. (1992) Correlation between phosphorylation of the chemotaxis protein CheY and its activity at the flagellar motor, *Biochemistry 31*, 1821-6.

20 Alon, U., Camarena, L., Surette, M. G., Aguera y Arcas, B., Liu, Y., Leibler, S., and Stock, J. B. (1998) Response regulator output in bacterial chemotaxis, *Embo J 17*, 4238-48.

21 Kuo, S. C., and Koshland, D. E., Jr. (1989) Multiple kinetic states for the flagellar motor switch, *J Bacteriol 171*, 6279-87.

22 Cluzel, P., Surette, M., and Leibler, S. (2000) An ultrasensitive bacterial motor revealed by monitoring signaling proteins in single cells, *Science 287*, 1652-5.

23 Borkovich, K. A., and Simon, M. I. (1990) The dynamics of protein phosphorylation in bacterial chemotaxis, *Cell 63*, 1339-48.

24 Segall, J. E., Manson, M. D., and Berg, H. C. (1982) Signal processing times in

bacterial chemotaxis, *Nature 296*, 855-7.

25 Springer, M. S., Goy, M. F., and Adler, J. (1979) Protein methylation in behavioural control mechanisms and in signal transduction, *Nature 280*, 279-84.

26 Block, S. M., Segall, J. E., and Berg, H. C. (1982) Impulse responses in bacterial chemotaxis, *Cell 31*, 215-26.

27 Komeda, Y. (1986) Transcriptional control of flagellar genes in *Escherichia coli* K-12, *J Bacteriol 168*, 1315-8.

28 Kutsukake, K., Ohya, Y., and Iino, T. (1990) Transcriptional analysis of the flagellar regulon of *Salmonella typhimurium*, *J Bacteriol 172*, 741-7.

29 Silverman, M., and Simon, M. (1974) Characterization of *Escherichia coli* flagellar mutants that are insensitive to catabolite repression, *J Bacteriol 120*, 1196-203.

30 Nishimura, A., and Hirota, Y. (1989) A cell division regulatory mechanism controls the flagellar regulon in *Escherichia coli*, *Mol Gen Genet 216*, 340-6.

31 Shi, W., Zhou, Y., Wild, J., Adler, J., and Gross, C. A. (1992) DnaK, DnaJ, and GrpE are required for flagellum synthesis in *Escherichia coli*, *J Bacteriol 174*, 6256-63.

32 Shin, S., and Park, C. (1995) Modulation of flagellar expression in *Escherichia coli* by acetyl phosphate and the osmoregulator OmpR, *J Bacteriol 177*, 4696-702.

33 Pruss, B. M., and Matsumura, P. (1996) A regulator of the flagellar regulon of *Escherichia coli*, flhD, also affects cell division, *J Bacteriol 178*, 668-74.

34 Hulko, M., Berndt, F., Gruber, M., Linder, J. U., Truffault, V., Schultz, A., Martin, J., Schultz, J. E., Lupas, A. N., and Coles, M. (2006) The HAMP domain structure implies helix rotation in transmembrane signaling, *Cell 126*, 929-40.

35 Kim, K. K., Yokota, H., and Kim, S. H. (1999) Four-helical-bundle structure of the cytoplasmic domain of a serine chemotaxis receptor, *Nature 400*, 787-92.

36 Ames, P., Studdert, C. A., Reiser, R. H., and Parkinson, J. S. (2002) Collaborative signaling by mixed chemoreceptor teams in *Escherichia coli*, *Proc Natl Acad Sci USA 99*, 7060-5.

37 Studdert, C. A., and Parkinson, J. S. (2005) Insights into the organization and dynamics of bacterial chemoreceptor clusters through in vivo crosslinking studies, *Proc Natl Acad Sci USA 102*, 15623-8.

38 Ames, P., and Parkinson, J. S. (2006) Conformational suppression of inter-receptor signaling defects, *Proc Natl Acad Sci USA 103*, 9292-7.

39 Studdert, C. A., and Parkinson, J. S. (2004) Crosslinking snapshots of bacterial chemoreceptor squads, *Proc Natl Acad Sci USA 101*, 2117-22.

40 Wu, J., Li, J., Li, G., Long, D. G., and Weis, R. M. (1996) The receptor binding site for the methyltransferase of bacterial chemotaxis is distinct from the sites of methylation, *Biochemistry 35*, 4984-93.

41 Djordjevic, S., and Stock, A. M. (1998) Chemotaxis receptor recognition by protein methyltransferase CheR, *Nat Struct Biol 5*, 446-50.

42 Barnakov, A. N., Barnakova, L. A., and Hazelbauer, G. L. (1999) Efficient adaptational demethylation of chemoreceptors requires the same enzyme-docking site as efficient methylation, *Proc Natl Acad Sci USA 96*, 10667-72.

43 Okumura, H., Nishiyama, S., Sasaki, A., Homma, M., and Kawagishi, I. (1998) Chemotactic adaptation is altered by changes in the carboxy-terminal sequence conserved among the major methyl-accepting chemoreceptors, *J Bacteriol 180*, 1862-8.

44 Sourjik, V., and Berg, H. C. (2002) Receptor sensitivity in bacterial chemotaxis, *Proc Natl Acad Sci USA 99*, 123-7.

45 Mao, H., Cremer, P. S., and Manson, M. D. (2003) A sensitive, versatile microfluidic assay for bacterial chemotaxis, *Proc Natl Acad Sci USA 100*, 5449-54.

46 Berg, H. C., and Tedesco, P. M. (1975) Transient response to chemotactic stimuli in *Escherichia coli*, *Proc Natl Acad Sci USA 72*, 3235-9.

47 Mesibov, R., Ordal, G. W., and Adler, J. (1973) The range of attractant concentrations for bacterial chemotaxis and the threshold and size of response over this range. Weber law and related phenomena, *J Gen Physiol 62*, 203-23.

48 Koshland, D. E., Jr., Goldbeter, A., and Stock, J. B. (1982) Amplification and adaptation in regulatory and sensory systems, *Science 217*, 220-5.

49 Maddock, J. R., and Shapiro, L. (1993) Polar location of the chemoreceptor complex in the *Escherichia coli* cell, *Science 259*, 1717-23.

50 Lybarger, S. R., and Maddock, J. R. (2000) Differences in the polar clustering of the high- and low-abundance chemoreceptors of *Escherichia coli*, *Proc Natl Acad Sci USA 97*, 8057-62.

51 Sourjik, V., and Berg, H. C. (2000) Localization of components of the chemotaxis machinery of *Escherichia coli* using fluorescent protein fusions, *Mol Microbiol 37*, 740-51.

52 Lybarger, S. R., and Maddock, J. R. (1999) Clustering of the chemoreceptor complex in *Escherichia coli* is independent of the methyltransferase CheR and the methylesterase CheB, *J Bacteriol 181*, 5527-9.

53 Shimizu, T. S., Le Novere, N., Levin, M. D., Beavil, A. J., Sutton, B. J., and Bray, D. (2000) Molecular model of a lattice of signalling proteins involved in bacterial chemotaxis, *Nat Cell Biol 2*, 792-6.

54 Shrout, A. L., Montefusco, D. J., and Weis, R. M. (2003) Template-directed assembly of receptor signaling complexes, *Biochemistry 42*, 13379-85.

55 Asinas, A. E., and Weis, R. M. (2006) Competitive and cooperative interactions in receptor signaling complexes, *J Biol Chem 281*, 30512-23.

56 Feng, X., Lilly, A. A., and Hazelbauer, G. L. (1999) Enhanced function conferred on low-abundance chemoreceptor Trg by a methyltransferase-docking site, *J Bacteriol 181*, 3164-71.

57 Blair, D. F. (1995) How bacteria sense and swim, *Annu Rev Microbiol 49*, 489-522.

58 Falke, J. J., and Hazelbauer, G. L. (2001) Transmembrane signaling in bacterial chemoreceptors, *Trends Biochem Sci 26*, 257-65.

59 Robinson, V. L., Buckler, D. R., and Stock, A. M. (2000) A tale of two components: a novel kinase and a regulatory switch, *Nat Struct Biol 7*, 626-33.

60 Sourjik, V. (2004) Receptor clustering and signal processing in *E. coli* chemotaxis, *Trends Microbiol 12*, 569-76.

61 Borkovich, K. A., Kaplan, N., Hess, J. F., and Simon, M. I. (1989) Transmembrane signal transduction in bacterial chemotaxis involves ligand-dependent activation of phosphate group transfer, *Proc Natl Acad Sci USA 86*, 1208-12.

62 Alley, M. R., Maddock, J. R., and Shapiro, L. (1992) Polar localization of a bacterial chemoreceptor, *Genes Dev 6*, 825-36.

63 Harrison, D. M., Skidmore, J., Armitage, J. P., and Maddock, J. R. (1999) Localization and environmental regulation of MCP-like proteins in *Rhodobacter sphaeroides*, *Mol Microbiol 31*, 885-92.

64 Francis, N. R., Levit, M. N., Shaikh, T. R., Melanson, L. A., Stock, J. B., and DeRosier, D. J. (2002) Subunit organization in a soluble complex of tar, CheW, and CheA by electron microscopy, *J Biol Chem 277*, 36755-9.

65 Segall, J. E., Block, S. M., and Berg, H. C. (1986) Temporal comparisons in bacterial chemotaxis, *Proc Natl Acad Sci USA 83*, 8987-91.

66 Bray, D., Levin, M. D., and Morton-Firth, C. J. (1998) Receptor clustering as a cellular mechanism to control sensitivity, *Nature 393*, 85-8.

67 Duke, T. A., and Bray, D. (1999) Heightened sensitivity of a lattice of membrane receptors, *Proc Natl Acad Sci USA 96*, 10104-8.

68 Duke, T. A., Le Novere, N., and Bray, D. (2001) Conformational spread in a ring of proteins: a stochastic approach to allostery, *J Mol Biol 308*, 541-53.

69 Shimizu, T. S., Aksenov, S. V., and Bray, D. (2003) A spatially extended

stochastic model of the bacterial chemotaxis signalling pathway, *J Mol Biol 329*, 291-309.

70 Albert, R., Chiu, Y. W., and Othmer, H. G. (2004) Dynamic receptor team formation can explain the high signal transduction gain in *Escherichia coli*, *Biophys J 86*, 2650-9.

71 Sourjik, V., and Berg, H. C. (2004) Functional interactions between receptors in bacterial chemotaxis, *Nature 428*, 437-41.

72 Gestwicki, J. E., and Kiessling, L. L. (2002) Inter-receptor communication through arrays of bacterial chemoreceptors, *Nature 415*, 81-4.

73 Smith, R. A., and Parkinson, J. S. (1980) Overlapping genes at the cheA locus of *Escherichia coli*, *Proc Natl Acad Sci USA 77*, 5370-4.

74 Parkinson, J. S., and Houts, S. E. (1982) Isolation and behavior of *Escherichia coli* deletion mutants lacking chemotaxis functions, *J Bacteriol 151*, 106-13.

75 Studier, F. W., and Moffatt, B. A. (1986) Use of bacteriophage T7 RNA polymerase to direct selective high-level expression of cloned genes, *J Mol Biol 189*, 113-30.

76 Rosenberg, A. H., Lade, B. N., Chui, D. S., Lin, S. W., Dunn, J. J., and Studier, F. W. (1987) Vectors for selective expression of cloned DNAs by T7 RNA polymerase, *Gene 56*, 125-35.

77 Garzon, A., and Parkinson, J. S. (1996) Chemotactic signaling by the P1 phosphorylation domain liberated from the CheA histidine kinase of *Escherichia coli*, *J Bacteriol 178*, 6752-8.

78 Guzman, L. M., Belin, D., Carson, M. J., and Beckwith, J. (1995) Tight regulation, modulation, and high-level expression by vectors containing the arabinose PBAD promoter, *J Bacteriol 177*, 4121-30.

79 Beverin, S., Sheppard, D. E., and Park, S. S. (1971) D-Fucose as a gratuitous inducer of the L-arabinose operon in strains of *Escherichia coli* B-r mutant in gene araC, *J Bacteriol 107*, 79-86.

80 Huang, W., McKevitt, M., and Palzkill, T. (2000) Use of the arabinose p(bad) promoter for tightly regulated display of proteins on bacteriophage, *Gene 251*, 187-97.

81 Matsumura, P., Rydel, J. J., Linzmeier, R., and Vacante, D. (1984) Overexpression and sequence of the *Escherichia coli* cheY gene and biochemical activities of the CheY protein, *J Bacteriol 160*, 36-41.

82 Miller, J. H. (1972) *Experiments in Molecular Genetics*, Cold Spring Harbor Laboratory, Cold Spring Harbor, New York.

83 Hess, J. F., Bourret, R. B., and Simon, M. I. (1991) Phosphorylation assays for proteins of the two-component regulatory system controlling chemotaxis in *Escherichia coli*, *Methods Enzymol 200*, 188-204.

84 Bradford, M. M. (1976) A rapid and sensitive method for the quantitation of microgram quantities of protein utilizing the principle of protein-dye binding, *Anal Biochem 72*, 248-54.

85 Osborn, M. J., and Munson, R. (1974) Separation of the inner (cytoplasmic) and outer membranes of Gram-negative bacteria, *Methods Enzymol 31*, 642-53.

86 Borkovich, K. A., and Simon, M. I. (1991) Coupling of receptor function to phosphate-transfer reactions in bacterial chemotaxis, *Methods Enzymol 200*, 205-14.

87 Bornhorst, J. A., and Falke, J. J. (2000) Attractant regulation of the aspartate receptor-kinase complex: limited cooperative interactions between receptors and effects of the receptor modification state, *Biochemistry 39*, 9486-93.

88 Evans, M. H., N.; and Peacock, B. (2000) *Statistical Distribution*, 3rd ed., Wiley, New York.

89 Lai, R. Z., Manson, J. M., Bormans, A. F., Draheim, R. R., Nguyen, N. T., and Manson, M. D. (2005) Cooperative Signaling among Bacterial Chemoreceptors, *Biochemistry 44*, 14298-307.

90 Gegner, J. A., Graham, D. R., Roth, A. F., and Dahlquist, F. W. (1992) Assembly of an MCP receptor, CheW, and kinase CheA complex in the bacterial

chemotaxis signal transduction pathway, *Cell 70*, 975-82.

91 Li, G., and Weis, R. M. (2000) Covalent modification regulates ligand binding to receptor complexes in the chemosensory system of *Escherichia coli*, *Cell 100*, 357-65.

92 Lefman, J., Zhang, P., Hirai, T., Weis, R. M., Juliani, J., Bliss, D., Kessel, M., Bos, E., Peters, P. J., and Subramaniam, S. (2004) Three-dimensional electron microscopic imaging of membrane invaginations in *Escherichia coli* overproducing the chemotaxis receptor Tsr, *J Bacteriol 186*, 5052-61.

93 Baumgartner, J. W., Kim, C., Brissette, R. E., Inouye, M., Park, C., and Hazelbauer, G. L. (1994) Transmembrane signalling by a hybrid protein: communication from the domain of chemoreceptor Trg that recognizes sugar-binding proteins to the kinase/phosphatase domain of osmosensor EnvZ, *J Bacteriol 176*, 1157-63.

94 Feng, X., Baumgartner, J. W., and Hazelbauer, G. L. (1997) High- and low-abundance chemoreceptors in *Escherichia coli*: differential activities associated with closely related cytoplasmic domains, *J Bacteriol 179*, 6714-20.

95 Weerasuriya, S., Schneider, B. M., and Manson, M. D. (1998) Chimeric chemoreceptors in *Escherichia coli*: signaling properties of Tar-Tap and Tap-Tar hybrids, *J Bacteriol 180*, 914-20.

96 Falke, J. J., Bass, R. B., Butler, S. L., Chervitz, S. A., and Danielson, M. A. (1997) The two-component signaling pathway of bacterial chemotaxis: a molecular view of signal transduction by receptors, kinases, and adaptation enzymes, *Annu Rev Cell Dev Biol 13*, 457-512.

97 Ravid, S., Matsumura, P., and Eisenbach, M. (1986) Restoration of flagellar clockwise rotation in bacterial envelopes by insertion of the chemotaxis protein CheY, *Proc Natl Acad Sci USA 83*, 7157-61.

98 Welch, M., Oosawa, K., Aizawa, S., and Eisenbach, M. (1993) Phosphorylation-dependent binding of a signal molecule to the flagellar switch of bacteria, *Proc Natl Acad Sci USA 90*, 8787-91.

99 Stock, J. B., and Koshland, D. E., Jr. (1978) A protein methylesterase involved in

bacterial sensing, *Proc Natl Acad Sci USA 75*, 3659-63.

100 Goy, M. F., Springer, M. S., and Adler, J. (1977) Sensory transduction in *Escherichia coli*: role of a protein methylation reaction in sensory adaptation, *Proc Natl Acad Sci USA 74*, 4964-8.

101 Barnakov, A. N., Barnakova, L. A., and Hazelbauer, G. L. (2001) Location of the receptor-interaction site on CheB, the methylesterase response regulator of bacterial chemotaxis, *J Biol Chem 276*, 32984-9.

102 Hazelbauer, G. L., and Engstrom, P. (1981) Multiple forms of methyl-accepting chemotaxis proteins distinguished by a factor in addition to multiple methylation, *J Bacteriol 145*, 35-42.

103 Wang, E. A., Mowry, K. L., Clegg, D. O., and Koshland, D. E., Jr. (1982) Tandem duplication and multiple functions of a receptor gene in bacterial chemotaxis, *J Biol Chem 257*, 4673-6.

104 Krikos, A., Mutoh, N., Boyd, A., and Simon, M. I. (1983) Sensory transducers of *E. coli* are composed of discrete structural and functional domains, *Cell 33*, 615-22.

105 Falke, J. J., and Kim, S. H. (2000) Structure of a conserved receptor domain that regulates kinase activity: the cytoplasmic domain of bacterial taxis receptors, *Curr Opin Struct Biol 10*, 462-9.

106 Butler, S. L., and Falke, J. J. (1998) Cysteine and disulfide scanning reveals two amphiphilic helices in the linker region of the aspartate chemoreceptor, *Biochemistry 37*, 10746-56.

107 Williams, S. B., and Stewart, V. (1999) Functional similarities among two-component sensors and methyl-accepting chemotaxis proteins suggest a role for linker region amphipathic helices in transmembrane signal transduction, *Mol Microbiol 33*, 1093-102.

108 Aravind, L., and Ponting, C. P. (1999) The cytoplasmic helical linker domain of receptor histidine kinase and methyl-accepting proteins is common to many prokaryotic signalling proteins, *FEMS Microbiol Lett 176*, 111-6.

109 Changeux, J. P., and Edelstein, S. J. (2005) Allosteric mechanisms of signal transduction, *Science 308*, 1424-8.

110 Falke, J. J., and Koshland, D. E., Jr. (1987) Global flexibility in a sensory receptor: a site-directed cross-linking approach, *Science 237*, 1596-600.

111 Boukhvalova, M. S., Dahlquist, F. W., and Stewart, R. C. (2002) CheW binding interactions with CheA and Tar. Importance for chemotaxis signaling in *Escherichia coli*, *J Biol Chem 277*, 22251-9.

112 Russo, A. F., and Koshland, D. E., Jr. (1983) Separation of signal transduction and adaptation functions of the aspartate receptor in bacterial sensing, *Science 220*, 1016-20.

113 Terwilliger, T. C., Wang, J. Y., and Koshland, D. E., Jr. (1986) Kinetics of receptor modification. The multiply methylated aspartate receptors involved in bacterial chemotaxis, *J Biol Chem 261*, 10814-20.

114 Draheim, R. R., Bormans, A. F., Lai, R. Z., and Manson, M. D. (2005) Tryptophan residues flanking the second transmembrane helix (TM2) set the signaling state of the Tar chemoreceptor, *Biochemistry 44*, 1268-77.

115 Stock, A., Schaeffer, E., Koshland, D. E., Jr., and Stock, J. (1987) A second type of protein methylation reaction in bacterial chemotaxis, *J Biol Chem 262*, 8011-4.

116 Li, M., and Hazelbauer, G. L. (2006) The carboxyl-terminal linker is important for chemoreceptor function, *Mol Microbiol 60*, 469-79.

117 Rebbapragada, A., Johnson, M. S., Harding, G. P., Zuccarelli, A. J., Fletcher, H. M., Zhulin, I. B., and Taylor, B. L. (1997) The Aer protein and the serine chemoreceptor Tsr independently sense intracellular energy levels and transduce oxygen, redox, and energy signals for *Escherichia coli* behavior, *Proc Natl Acad Sci USA 94*, 10541-6.

118 Milburn, M. V., Prive, G. G., Milligan, D. L., Scott, W. G., Yeh, J., Jancarik, J., Koshland, D. E., Jr., and Kim, S. H. (1991) Three-dimensional structures of the ligand-binding domain of the bacterial aspartate receptor with and without a ligand, *Science 254*, 1342-7.

119 Jeffery, C. J., and Koshland, D. E., Jr. (1993) Three-dimensional structural model of the serine receptor ligand-binding domain, *Protein Sci 2*, 559-66.

120 Zhulin, I. B., Nikolskaya, A. N., and Galperin, M. Y. (2003) Common extracellular sensory domains in transmembrane receptors for diverse signal transduction pathways in bacteria and archaea, *J Bacteriol 185*, 285-94.

121 Chervitz, S. A., Lin, C. M., and Falke, J. J. (1995) Transmembrane signaling by the aspartate receptor: engineered disulfides reveal static regions of the subunit interface, *Biochemistry 34*, 9722-33.

122 Hughson, A. G., and Hazelbauer, G. L. (1996) Detecting the conformational change of transmembrane signaling in a bacterial chemoreceptor by measuring effects on disulfide cross-linking in vivo, *Proc Natl Acad Sci USA 93*, 11546-51.

123 Ottemann, K. M., Xiao, W., Shin, Y. K., and Koshland, D. E., Jr. (1999) A piston model for transmembrane signaling of the aspartate receptor, *Science 285*, 1751-4.

124 Isaac, B., Gallagher, G. J., Balazs, Y. S., and Thompson, L. K. (2002) Site-directed rotational resonance solid-state NMR distance measurements probe structure and mechanism in the transmembrane domain of the serine bacterial chemoreceptor, *Biochemistry 41*, 3025-36.

125 Miller, A. S., and Falke, J. J. (2004) Side chains at the membrane-water interface modulate the signaling state of a transmembrane receptor, *Biochemistry 43*, 1763-70.

126 Liu, J. D., and Parkinson, J. S. (1991) Genetic evidence for interaction between the CheW and Tsr proteins during chemoreceptor signaling by *Escherichia coli*, *J Bacteriol 173*, 4941-51.

127 Levit, M. N., Grebe, T. W., and Stock, J. B. (2002) Organization of the receptor-kinase signaling array that regulates *Escherichia coli* chemotaxis, *J Biol Chem 277*, 36748-54.

128 Le Moual, H., and Koshland, D. E., Jr. (1996) Molecular evolution of the C-terminal cytoplasmic domain of a superfamily of bacterial receptors involved in taxis, *J Mol Biol 261*, 568-85.

129 Lai, W. C., and Hazelbauer, G. L. (2005) Carboxyl-terminal extensions beyond the conserved pentapeptide reduce rates of chemoreceptor adaptational modification, *J Bacteriol 187*, 5115-21.

130 Le Moual, H., Quang, T., and Koshland, D. E., Jr. (1997) Methylation of the *Escherichia coli* chemotaxis receptors: intra- and interdimer mechanisms, *Biochemistry 36*, 13441-8.

131 Li, J., Li, G., and Weis, R. M. (1997) The serine chemoreceptor from *Escherichia coli* is methylated through an inter-dimer process, *Biochemistry 36*, 11851-7.

132 Kim, S. H., Wang, W., and Kim, K. K. (2002) Dynamic and clustering model of bacterial chemotaxis receptors: structural basis for signaling and high sensitivity, *Proc Natl Acad Sci USA 99*, 11611-5.

133 Starrett, D. J., and Falke, J. J. (2005) Adaptation mechanism of the aspartate receptor: electrostatics of the adaptation subdomain play a key role in modulating kinase activity, *Biochemistry 44*, 1550-60.

134 Bechinger, B., Kinder, R., Helmle, M., Vogt, T. C., Harzer, U., and Schinzel, S. (1999) Peptide structural analysis by solid-state NMR spectroscopy, *Biopolymers 51*, 174-90.

135 Hosking, E. R., Vogt, C., Bakker, E. P., and Manson, M. D. (2006) The *Escherichia coli* MotAB proton channel unplugged, *J Mol Biol 364*, 921-37.

136 Manson, M. D., Boos, W., Bassford, P. J., Jr., and Rasmussen, B. A. (1985) Dependence of maltose transport and chemotaxis on the amount of maltose-binding protein, *J Biol Chem 260*, 9727-33.

137 Morton-Firth, C. J., Shimizu, T. S., and Bray, D. (1999) A free-energy-based stochastic simulation of the Tar receptor complex, *J Mol Biol 286*, 1059-74.

138 Mello, B. A., and Tu, Y. (2005) An allosteric model for heterogeneous receptor complexes: understanding bacterial chemotaxis responses to multiple stimuli, *Proc Natl Acad Sci USA 102*, 17354-9.

139 Ames, P., and Parkinson, J. S. (1988) Transmembrane signaling by bacterial chemoreceptors: E. coli transducers with locked signal output, *Cell 55*, 817-26.

140 Altschuh, D., Oncul, S., and Demchenko, A. P. (2006) Fluorescence sensing of intermolecular interactions and development of direct molecular biosensors, *J Mol Recognit 19*, 459-77.

141 Jurss, R., Prinz, H., and Maelicke, A. (1979) NBD-5-acylcholine: fluorescent analog of acetylcholine and agonist at the neuromuscular junction, *Proc Natl Acad Sci USA 76*, 1064-8.

VITA

Name: Runzhi Lai

Address: Biology Department, BSBE 303
MS 3258
Texas A&M University
College Station, TX 77843

Email: RunzhiLai@gmail.com

Education: B.S. in Biotechnology, Huazhong Agricultural University, P. R. China
Ph.D. in Microbiology, Texas A&M University